AUTHOR QUERY FORM

	Journal: DIFF **Article Number: 342**	**Please e-mail or fax your responses and any corrections to:** **E-mail: corrections.eseo@elsevier.macipd.com** **Fax: +44 1392 285878**

Dear Author,

Please check your proof carefully and mark all corrections at the appropriate place in the proof (e.g., by using on-screen annotation in the PDF file) or compile them in a separate list. Note: if you opt to annotate the file with software other than Adobe Reader then please also highlight the appropriate place in the PDF file. To ensure fast publication of your paper please return your corrections within 48 hours.

For correction or revision of any artwork, please consult http://www.elsevier.com/artworkinstructions.

Any queries or remarks that have arisen during the processing of your manuscript are listed below and highlighted by flags in the proof. Click on the Q link to go to the location in the proof.
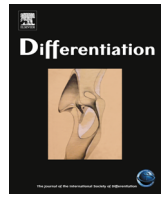
Location in article	Query / Remark: **click on the Q link to go** **Please insert your reply or correction at the corresponding line in the proof**
Q1	Please confirm that given names and surnames have been identified correctly and are presented in the desired order.
Q2	Please complete and update the reference given here (preferably with a DOI if the publication data are not known): Dalcq, J., (in press). For references to articles that are to be included in the same (special) issue, please add the words 'this issue' wherever this occurs in the list and, if appropriate, in the text.
Q3	"Dalcq et al. (2012)" has been changed to "Dalcq et al. (in press)" as per the reference list. Please confirm.
Q4	The decimal comma has been changed to a decimal point in the given sentence "Morpholinos were diluted...". Please check, and correct if necessary.

Thank you for your assistance.

<div style="border:1px solid black">
Please check this box or indicate your approval
if you have no corrections to make to the PDF file
</div>

Highlights

Differentiation ∎ (∎∎∎∎) ∎∎∎–∎∎∎

Fgf receptors Fgfr1a and Fgfr2 control the function of pharyngeal endoderm in late cranial cartilage development

Q1

Arnaud Larbuisson, Julia Dalcq, Joseph A. Martial, Marc Muller

Laboratory for Molecular Biology and Genetic Engineering, GIGA-R, Université de Liège, B34, Liège, Belgium

- The Fgf pathway is required around 30 hpf for head cartilage formation.
- Receptors Fgfr1a and Fgfr2 are expressed in pharyngeal endoderm beyond 26 hpf.
- Fgf signaling initiates a Runx3, Egr1, Sox9b regulatory cascade in pharyngeal endoderm.
- Fgfr1a and Fgfr2 are required for repression of the BMP inhibitor follistatin A.
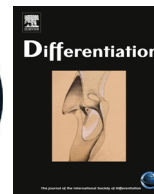
Fgf receptors Fgfr1a and Fgfr2 control the function of pharyngeal endoderm in late cranial cartilage development

Arnaud Larbuisson, Julia Dalcq, Joseph A. Martial, Marc Muller*

Laboratory for Molecular Biology and Genetic Engineering, GIGA-R, Université de Liège, B34, Liège, Belgium

A B S T R A C T

Cranial cartilage derives mainly from cranial neural crest cells and its formation requires fibroblast growth factor (Fgf) signaling for early differentiation and survival of developing chondrocytes as well as patterning of the endodermal pouches.

Here, we investigate the role of Fgf receptors in chondrocyte maturation at later stages, beyond 24 hpf. Using inducible expression of a dominant-negative Fgf receptor, we show that Fgf signaling is required around 30 hpf for correct cartilage formation. The receptor genes *fgfr1a* and *fgr2* are expressed in pharyngeal endodermal pouches after 24 hpf or 26 hpf, respectively. Depletion of any of these two receptors by microinjection of antisense morpholinos results in severe defects in cartilage formation at 4 dpf and a decrease in expression of the late chondrocyte markers *barx1* and *runx2b*. Although endodermal pouches are correctly formed and patterned, receptor knock down leads to decreased expression of *runx3*, *egr1* and *sox9b* in this tissue, while expression of *fsta*, coding for a secreted BMP/Tgfß inhibitor, is clearly increased. Rescue experiments revealed that each Fgfr1a or Fgfr2 receptor is able to compensate for the loss of the other.

Thus, we show that minimal amounts of Fgfr1a or Fgfr2 are required to initiate a regulatory cascade in pharyngeal endoderm reducing expression of *fsta*, thereby allowing correct BMP signaling to the maturing chondrocytes of the head cartilage.

© 2013 Published by Elsevier B.V. on behalf of International Society of Differentiation

1. Introduction

Craniofacial bone structures result from both membranous and endochondral or perichondral ossification, the latter requiring preliminary formation of a cartilaginous matrix. Pharyngeal cartilages derive from migration and differentiation of cranial neural crest cells (cNCC) within the pharyngeal arches. These cNCCs are formed at the neurulation stage and migrate in three streams into the seven pharyngeal pouches to form the different cartilage elements of the viscerocranium (mandible, hyoid, five ceratobranchial arches) (Schilling and Kimmel, 1994; Knight and Schilling, 2006). During and after this migration, the cNCCs undergo several differentiation steps to finally give rise to hypertrophic chondrocytes and osteogenic cells. After initial expression of *tfap2a* characteristic to all cNCC cells (Barrallo-Gimeno et al., 2004), ectomesenchymal cartilage precursors are identified by early expression of *dlx2a* (Sperber et al., 2008) while chondrogenic differentiation is characterized by the onset of *sox9a* expression required for production of the cartilage-specific collagen Col2a1 (Kluver et al., 2005; Yan et al., 2005). Finally, maturing hypertrophic chondrocytes express *runx2b* (Flores et al., 2008; Flores et al., 2004), a marker that is also present in bone-forming osteoblasts.

In the arches, the cNCCs are surrounded by and interact with different tissues such as pharyngeal endoderm and ectodermal epithelium. In *casanova* (*cas*) mutant zebrafish, endoderm is lacking (Alexander et al., 1999) and pharyngeal cartilages are not formed (David et al., 2002). Loss of function of several genes expressed in pharyngeal endoderm, such as *egr1*, *runx3* or *sox9b* leads to severe reduction of head cartilage at 4 dpf (Dalcq et al., in press; Kluver et al., 2005; Yan et al., 2005; Flores et al., 2006). Thus, interaction between endoderm and cNCCs is primordial for the correct formation of pharyngeal cartilage (Crump et al., 2004; Piotrowski and Nusslein-Volhard, 2000; Schilling et al., 1996) involving signaling pathways initiated by Bmp, Fgf or Hh ligands (Goldring et al., 2006; Walshe and Mason, 2003). Recently, BMP signaling was shown to be required for early ventral arch development, upstream and simultaneously to endothelin1 (Edn1) (Alexander et al., 2011). An additional role for craniofacial patterning at later stages was also shown. We recently showed the existence of a regulatory cascade formed by the three transcription factors Runx3–Egr1–Sox9b, each being required for expression of the next, in pharyngeal endoderm at 30 hpf (Dalcq et al., in press).

* Corresponding author. Tel.: +32 4 366 4437; fax: +32 4 366 4198.
E-mail address: m.muller@ulg.ac.be (M. Muller).

This cascade controls late chondrogenesis by down-regulating expression of Follistatin A (*fsta*), a known antagonist of BMP signaling, thereby allowing correct activation of the BMP pathway required to activate *runx2b* expression in developing chondrocytes.

Fibroblast growth factor (Fgf) signaling is involved in proliferation, migration and specification of many cell types (Ornitz and Itoh, 2001; Walshe and Mason, 2003; Thisse and Thisse, 2005). It is highly conserved across different species (Itoh, 2007; Itoh and Ornitz, 2008) and is initiated by numerous Fgf ligands binding specific tyrosine kinase (RTK) receptors (Fgfrs). In mice, Fgf9 controls early hypertrophic chondrocyte differentiation (Hung et al., 2007) while in zebrafish, Fgf3 and Fgf8 are produced in pharyngeal endoderm and ectoderm and control segmentation of the pharyngeal endoderm and survival of cNCCs (Crump et al., 2004; David et al., 2002; Walshe and Mason, 2003). Five genes for Fgfrs have been identified: Fgfr1-4 (RTK) and Fgfr5/Fgfrl1. In Fgfrl1, the tyrosine kinase domain is replaced by a phosphatase domain: it thus acts as a negative regulator of Fgf signaling (Hall et al., 2006) and is also important for craniofacial cartilage formation (Hall et al., 2006; Trueb and Taeschler, 2006). In humans, mutations in Fgfrs, causing either increased or decreased Fgf signaling, generate craniofacial malformations resulting from deficient chondrogenesis (*e.g.* Apert syndrome, Crouzon syndrome, Pfeiffer syndrome, Kallmann syndrome 2, Jackson–Weiss syndrome) (Nie et al., 2006; Baldridge et al., 2010). In mice, *fgfr1* controls endoderm patterning in the pharyngeal region and plays a crucial role in cNCC migration into the branchial arches (Trokovic et al., 2003). Different studies in zebrafish have shown that inhibition of Fgfr signaling by SU5402 generates embryos lacking pharyngeal cartilage at 4 days post fertilization (dpf) and down-regulates expression of genes known to be crucial for chondrogenesis (Walshe and Mason, 2003; Sperber et al., 2008).

In zebrafish, the role of Fgf signaling in head cartilage formation was mainly studied by blocking the pathway at very early stages and thus possibly affecting multiple functions of this versatile signaling during early development. Here, we used heat-shock controlled expression of a dominant-negative Fgf receptor in *Tg*(*hsp70l:dnfgfr1-EGFP*)*pd1* transgenic embryos to show a critical stage for Fgfr activities in chondrogenesis around 30 hpf. We also show that *fgfr1a* and *fgfr2* are both expressed in pharyngeal endoderm at this stage and we demonstrate that *fgfr1a* or *fgfr2* depletion specifically causes severe cartilage defects at 4 dpf, which can be rescued by concomitant expression of exogenous zebrafish or human Fgf receptors. We further show that these two receptors are required for activation of the Runx3–Egr1–Sox9b–Fsta cascade in the endoderm and for *runx2b* expression in developing chondrocytes. Finally, the defects in cartilage structure and gene expression observed in morphants for each of the receptors Fgfr1a or Fgfr2 can be rescued by ectopic expression of each of the two receptors, indicating that the exact identity of the receptor active in pharyngeal endoderm is not important, but rather the precise number of receptor molecules.

2. Materials and methods

2.1. Zebrafish maintenance and transgenic line

Adult zebrafish (*Danio rerio*) and embryos were raised as described (Westerfield, 2007). Embryos were kept in E3 medium at 28 °C and developed until the stages of interest according to Kimmel et al. (1995). The transgenic lines *Tg*(*hsp70l:dnfgfr1-EGFP*)*pd1* (Lee et al., 2005) and *Tg*(*sox17-GFP*)*s870* (Sakaguchi et al., 2006) were obtained from the ZIRC (Eugene, Oregon, USA).

2.2. Ethics statement

All experiments and the entire study were evaluated by the Ethical Committee of the University of Liege, Belgium and accepted under the file numbers 377, 568 and 1074.

2.3. Knockdown of fgfr1a and fgfr2

One to two cell-stage embryos were injected with 4 ng of antisense morpholino oligonucleotides (MO, Gene Tools Inc.) complementary to the translational start site of *fgfr1a* (tMOFgfr1: 5′-GCAGCAGCGTGGTCTTCATTATCAT-3′ (Scholpp et al., 2004) or its 5′ UTR: MOFgfr1a: 5′-CAAAGATCCTCTACATCTGAACTCC-3′ (Thummel et al., 2006). Splicing morpholinos targeting, respectively the second or first intron's donor splice site in the coding region of *fgfr1a* (5 ng; sMOFgfr1a: 5′-ATTCAGTTGCATTCTCACCTGTAAC-3′ (Nakayama et al., 2008)) or *fgfr2* (4 ng; MOFgfr2: 5′-GCTCAAATGTCTTACCTTCAGGTGC-3′ were also used. Co-injection of tMOFgfr1a and MOFgfr2 was performed with 2 ng of each morpholino. Morpholinos were diluted in Danieau buffer and Tetramethylrhodamine dextran (Invitrogen, Belgium) was added at 0.5% to verify proper injection of the embryos by fluorescence stereomicroscopy. Standard control morpholino (MOcon) was injected at the same concentrations. The efficacy of the sMOFgfr1a splicing morpholino was tested previously by RT-PCR (Nakayama et al., 2008), while that of sMOFgfr2 was confirmed using the oligonucleotides Fgfr2-MOtest-F: 5′-CTGCTAATGACCCTGGCAAC-3′ and Fgfr2-MOtest-R; 5′-AGCTGTCTTTGGTCCAGACG-3′ targeting, respectively exon 2 and exon 3. Injection of sMOFgfr2 led to alternative splicing resulting in deletion of 22 nucleotides at the end of exon 2, thus coding for a truncated and inactive protein (Movie 1 Fig. S1H). Although no increase of cell death was observed in the Fgfr1a morphants, in absence or presence of co-injection of a morpholino directed against p53, this MOp53 was co-injected in all knockdown experiments to ensure inhibition of MO-induced unspecific cell death (Robu et al., 2007). The effects of morpholino injection were tested on at least 150 individuals, performed in at least three independent experiments.

2.4. Rescue experiments

Human *FGFR1* mRNA was synthesized using mMessage mMachine Sp6 Kit (Ambion, TX, USA) from the IMAGE full length cDNA clone IRATp970D1237D (IMAGE ID: 3896359). The clone was digested using NotI. 80 pg of *FGFR1* mRNA was injected alone or co-injected with morpholino at the one-cell stage. *fgfr2* mRNA was obtained by digestion of the pZL1-zfgfr2 (ZDB-GENE-030323-1) clone by BamHI and synthesized using mMessage mMachine Sp6 Kit. 100 pg/egg of this mRNA were injected alone or with morpholino directed against Fgf receptors.

2.5. Whole-mount in situ hybridization

Wild type and injected embryos were raised in presence of 0.003% of 1-phenyl-2-thiourea (PTU) until the desired stages, fixed for 2 h in 4% PFA and dehydrated in 100% methanol for storage at −20 °C. Embryos were rehydrated in PBS and whole mount *in situ* hybridization was performed as described and adapted from Dalcq et al. (in press). Antisense probes were labeled with digoxigenin or DNP (2,4-dinitrophénol). Anti-digoxigenin-AP was used with NBT/BCIP for single *in situ* hybridization; anti-digoxigenin-HRP and anti-DNP-HRP were used with tyramide-Cy3 (Red) and tyramide-FITC (green) for the double fluorescent *in situ* hybridizations (Perkin-Elmer TSA Kit). The *fgfr1a* (ZDB-GENE-980526-255) and *fgfr2* (ZDB-GENE-030323-1) riboprobes were prepared from cDNA clones with Sp6 and T7 RNA polymerase. Other probes used were *barx1* (ZDB-GENE-050522-28) (Sperber and Dawid, 2008), *dlx2a*
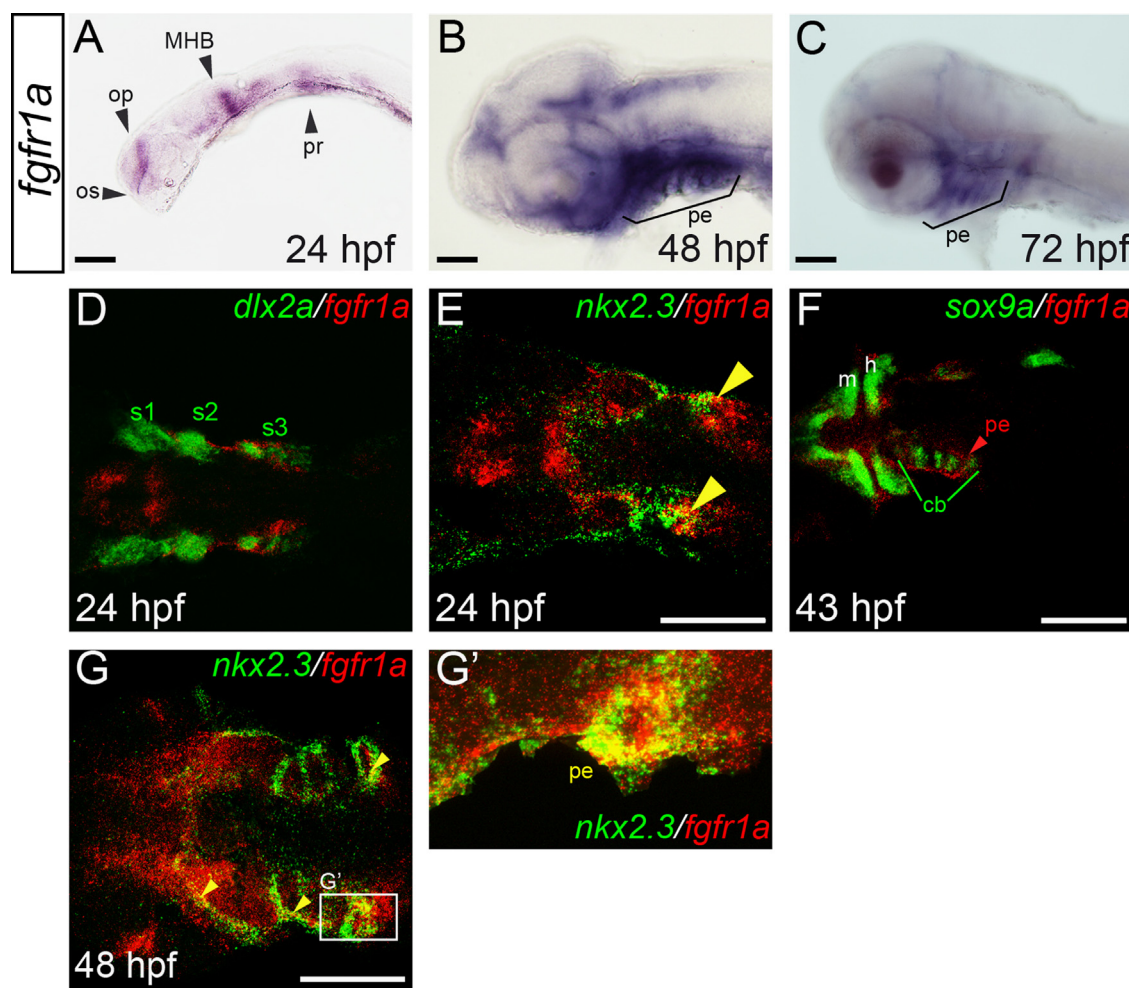
Fig. 1. *fgfr1a* is expressed in pharyngeal endoderm beyond 24 hpf. Simple *in situ* hybridization (ISH) using an *fgfr1a* probe of wt embryos at 24 (A), 48 (B) and 72 hpf (C); lateral views, anterior to the left. Single confocal sections of double fluorescent *in situ* hybridizations for expression of *fgfr1a* (red) and *dlx2a* (green) (D) or *nkx2.3* (green) (E) at 24 hpf; *sox9a* (green) at 43 hpf (F) or *nkx2.3* (green) at 48 hpf (G). (G′) confocal projection for *nkx2.3* (green) and *fgfr1a* (red) at 48 hpf in the domain delineated by the white rectangle in (G). Ventral views, anterior to the right (D–G′). *fgfr1a* expression is detected in the pharyngeal region (pr), the midbrain/hindbrain boundary (MHB), the optic stalk (os) and the olfactory placode (op) at 24 hpf (A). *fgfr1a* mRNA is still observed in brain and in the pharyngeal endoderm (pe) at 48 (B) and 72 hpf (C). In the pharyngeal region at 24 hpf, *fgfr1a* (red) expression domains surround those of *dlx2a* (green) (D), while they overlap with those of *nkx2.3* (green) cells in pharyngeal endoderm (E, yellow arrows). At 43 hpf, no colocalisation is observed between *sox9a* (green) and *fgfr1a* (red) (F). *fgfr1a* (red) continues to coexpressed with *nkx2.3* (green) in endodermal pouches (pe) at 48 hpf (G,G′; yellow arrows). Movies S1–S3: migration stream of cNCC. Scale bar: 150 μm.

(ZDB-GENE-980526-212) (Akimenko et al., 1994), *egr1* (ZDB-GENE-980526-320) (Close et al., 2002), *nkx2.3* (ZDB-GENE-990415-178) (Lee et al., 1996), *runx2b* and *runx3* (ZDB-GENE-040629-4 and ZDB-GENE-000605-2) (Flores et al., 2006), *sox9a* and *sox9b* (ZDB-GENE-001103-1 and -2) (Yan et al., 2005; Yan et al., 2002).

2.6. Alcian blue staining

To observe cartilage at 4 dpf, the embryos were stained with Alcian blue (Sigma, Bornem, Belgium) as described (Schilling et al., 1996).

2.7. Acridin orange staining

To detect unspecific cell death possibly due to morpholino injection, the treated larvae were exposed to a solution of acridin orange 5 μg/ml followed by 5 washing steps in E3 and finally observation of the fluorescent cells at 502 nm excitation.

2.8. Heatshock conditions

Tg(*hsp70l:dnfgfr1-EGFP*)*pd1* embryos were heat shocked during 30 min at the desired stages by transferring into preheated E3 at 37 °C in a water bath. After that, the embryos were returned to 28 °C until the desired stages were reached. After 24 h, the embryos were screened for GFP fluorescence to sort transgenic individuals from their non-transgenic siblings, only strongly fluorescent individuals were used for the experiment.

2.9. Immunohistochemistry for MAPK phosphorylation

For immunohistochemistry, embryos were fixed in 2% PFA/Pipes 0.1 M/MgSO$_4$ 1 mM/EGTA 2 mM, pH=7 over night at 4 °C. After washing with PBTr 0.3% (PBS with Triton X100 0.3%), embryos were permeabilized with acetone at −20 °C. Then, samples were washed 4 times in PBTr 0.3% and endogenous peroxidases were inhibited during 45 min with PBTr 0.3/H$_2$O$_2$ 2% followed by 4 washes in PBTr 0.3%. Finally, embryos were incubated in PBTr 0.3/4% BSA during 2 h at room temperature followed by incubation with P-MAPK antibodies 1/2000 in PBTr 0.3/4% BSA (Sigma M8159) over-night at 4 °C. Next, embryos were washed

6×30 min in PBTr 0.3 and incubated 1 h in PBTr 0.3/4% BSA. The blocking solution was replaced by blocking solution supplemented with a 500-fold dilution of the secondary antibody from Vectastain ABC Elite Mouse kit (Vector Laboratories) and incubated overnight at 4 °C. Then, embryos were washed 6 times for 30 min in PBTr 0.3. Next, they were incubated 1 h in A+B solutions from Vectastain Kit (15 µL/mL). After 3 washes of 15 min in PBTr 0.3, embryos were incubated in amplification diluent from TSA Molecular Probe kit (Perkin Elmer) for 5 min. Colorimetric staining was performed with Tyramide-FITC (1/1000) or Tyramide-Cy3 (1/500) in amplification diluent during 45 min at room temperature in the dark and, finally, the embryos were washed 5 times in PBTr 0.3.

2.10. Imaging and analysis

Visible *in situ* hybridization and Alcian blue pictures were acquired on a Nikon® ECLIPSE 90i microscope using NIS-Elements microscope imaging software. Fluorescent *in situ* images were captured on a Leica TCS SP2 confocal using LCS Leica SP2 software. Pictures and Z-stacks were analyzed with ImageJ; the same adjustments were used for all pictures from a same data group.

3. Results

3.1. fgfr1a and fgfr2 are expressed in pharyngeal endoderm.

Zebrafish *fgfr1a* expression was previously reported in brain, somites and in the pharyngeal region until 24 h post fertilization (Rohner et al., 2009; Schilling et al., 1996; Scholpp et al., 2004; Ota et al., 2010). We confirmed and analyzed more precisely *fgfr1a* expression in the pharyngeal region between 24 hpf and 72 hpf by simple ISH and by double fluorescent ISH with specific probes for *fgfr1a*, *dlx2a*, *nkx2.3* and *sox9a*. At 24 hpf, *fgfr1a* expression is observed in the Midbrain/Hindbrain Boundary (MHB), optic stalk, olfactory placode and pharyngeal region (Fig. 1A), as expected. Moreover, *fgfr1a* mRNA co localized with that for *nkx2.3* in pharyngeal endoderm at 24 hpf (yellow arrows; Fig. 1E; Movie S1), but scarcely with *dlx2a* mRNA in cranial neural crest cells (cNCC) (Fig. 1D; Movie S2); areas of *fgfr1a* expression in the pharyngeal region mainly surround those of *dlx2a*. At 43 hpf, the *sox9a* expression domain in cNCC is mainly surrounded by *fgfr1a* expression domains in the endodermal pouches (Fig. 1F; Movie S3). *fgfr1a* is still expressed at 48 hpf and 72 hpf in brain and in endodermal tissues (Fig. 1B, C, G, G′). Colocalisation of *nkx2.3* and *fgfr1a* expression at 48 hpf is apparent in endodermal pouches in the pharyngeal region (yellow arrows; Fig. 1G, G′; Movies S4 and S5).

Expression of *fgfr2* is detected in wild type 24 hpf embryos in hindbrain rhombomers (R1-4), the tectum, the optic stalk and olfactory placodes and weakly in the pharyngeal region (Fig. 2A). Expression increases in the pharyngeal region at 26 hpf in the most posterior arch and was present until 72 hpf (Fig. 2B–D), while its expression in the brain was maintained during these developmental stages. At 38 hpf, *fgfr2* mRNA was observed in the same cell type than *nkx2.3* i.e. in endodermal pouches of the pharyngeal region (yellow arrows; Fig. 2E; Movie S6). No coexpression of *fgfr2* mRNAs was observed with those of *sox9a* in cNCC of the pharyngeal region at 72 hpf (Fig. 2G; Movie S8); the *fgfr2* expression domains surround those for *sox9a* and correspond to pharyngeal endoderm. Double fluorescent ISH using probes for *fgfr1a* and *fgfr2* confirms co-expression of these two genes in endodermal pouches and in otic vesicles at 48 hpf (yellow; Fig. 2F; Movie S7).

In conclusion, both *fgfr1a* and *fgfr2* are predominantly expressed in cells of the pharyngeal endoderm.

3.2. Viscerocranium cartilage formation requires Fgf signaling beyond 24 hpf

To determine the importance of Fgf signaling specifically at stages beyond 24 hpf, we used *Tg*(*hsp70l:dnfgfr1-EGFP*)*pd1* transgenic embryos which express a dominant-negative Fgfr1 receptor under the control of the *hsp70l* heat shock promoter. We performed a heat shock for 30 min at different developmental stages between 24 and 48 hpf, thereby blocking Fgf signaling in the entire embryo. The embryos were left to develop until 4 days post fertilization (dpf) and head cartilage formation was assessed by alcian blue staining. We observed different phenotypes (Fig. 3A–F), ranging from close to wild type (type A), mildly affected cartilage with shortened mandible and hyoid (types B and C) through increasingly affected viscerocranium with a complete absence of ceratobranchials, a reduction of Meckel's cartilage and palatoquadrate, axis modification or absence of ceratohyoid (types D and E) to finally only remnants of the neurocranium (type F). Embryos that underwent heat shock at 26 or 30 hpf presented the highest proportion (Fig. 3G) of strongly affected cartilage structures. Heat shock treatments at earlier (before 25 hpf) or later stages (beyond 40 hpf) led to a lower proportion of highly affected larvae. The extent of MAPK phosphorylation was drastically reduced 15 h after heat shock treatment both at 24 and at 28 hpf (Movie S1, Fig. S1A–D), showing that Fgf signaling was similarly reduced in both cases. Siblings, identified as non-transgenic by the absence of GFP fluorescence formed normal head cartilage after any of the heat shock treatments, proving that the observed defects are indeed due to impairment of Fgf signaling by the transgene.

These observations indicate that Fgfr signaling plays a crucial role for pharyngeal cartilage formation between stages 26 and 40 hpf.

3.3. Both Fgfr1a and Fgfr2 receptors are required for cranial cartilage formation

To determine the effect of *fgfr1a* and *fgfr2* loss of function, we assessed cartilage formation in morpholino-injected larvae at 4 dpf by alcian blue staining. Injection of tMOFgfr1a, directed against the *fgfr1* translation initiation codon (Nakayama et al., 2008) caused an absence of ceratobranchial arches, a strong reduction of mandible size and inversion of the dorso-ventral axis of the hyoid in 49% ($n=185/377$) of observed individuals (Fig. 4A, B), as compared to embryos injected with control morpholino (MOcon). No difference was observed between injection of tMOFgfr1a and co-injection of a morpholino directed against p53 (MOp53), showing that the observed defects were not caused by unspecific apoptosis (not shown). In addition, no increase of apoptotic or necrotic cells was observed in the morphants by acridine orange staining, with or without co-injected MOp53 (not shown). Nevertheless, we performed all subsequent knock-down experiments by co injecting MOp53. To further confirm the specificity of the observed effects for Fgfr1a depletion, we co-injected tMOFgfr1a and mRNA coding for human FGFR1 into one-cell stage eggs. At 4 dpf, the proportion of strongly affected embryos had considerably decreaped, whereas 48% ($n=146/305$) of the embryos presented only slight modifications (Fig. 4C).

For further experiments, the alcian blue stained larvae were classified according to their cranial cartilage pattern, from wt (Type A, Fig. 5A), mildly affected (Fig. 5B), strongly affected head cartilage but with ceratobranchial arches still present (Fig. 5C), strongly affected and lacking ceratobranchial arches (Fig. 5D) to only remnants of the neurocranium (type E, Fig. 5E). Finally, type F
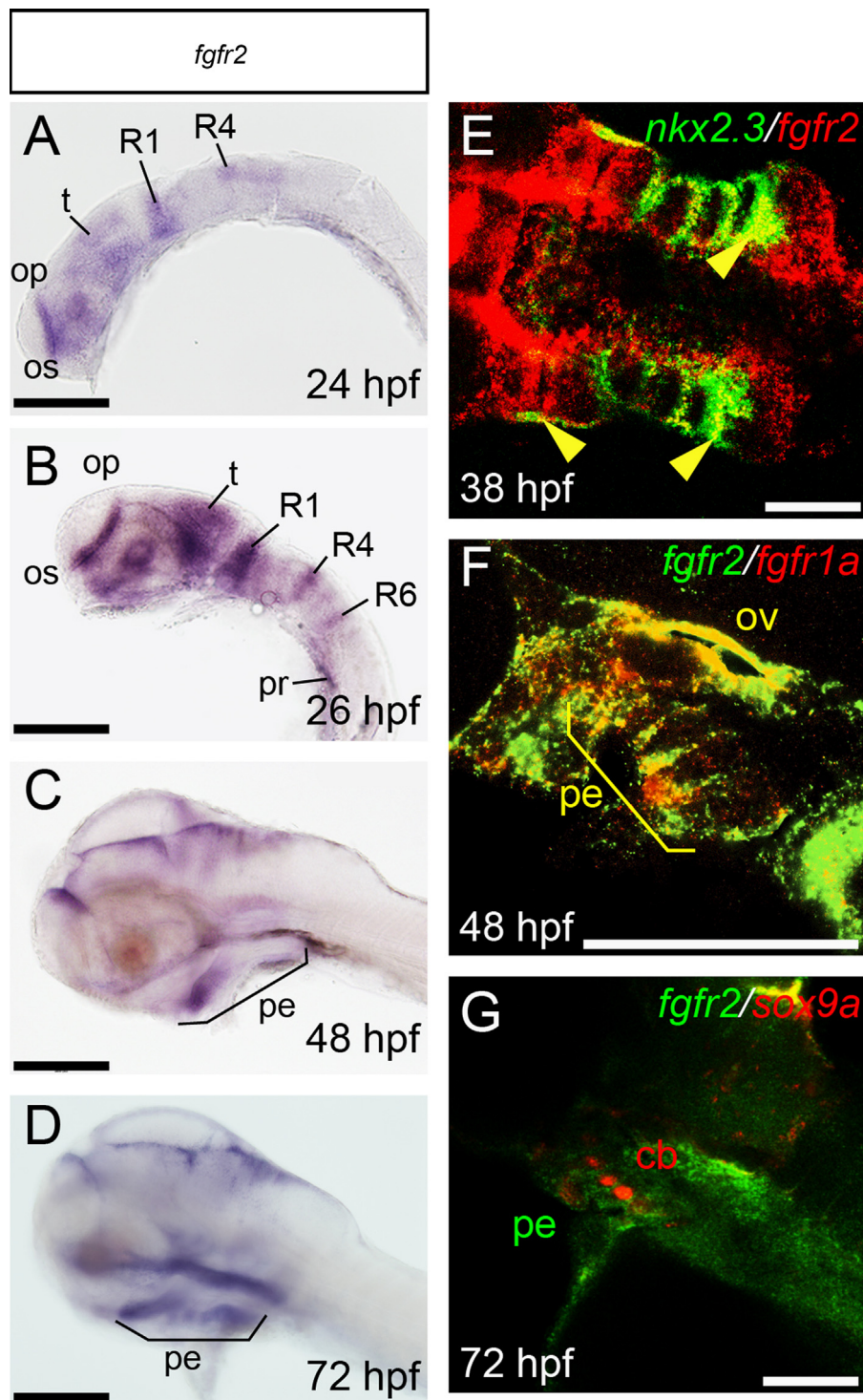
Fig. 2. *fgfr2* is expressed in pharyngeal endoderm starting at 26 hpf. Simple *in situ* hybridization for *fgfr2* of wt embryos at 24 hpf (A), 26 hpf (B), 48 hpf (C) and 72 hpf (D). Lateral views, anterior to the left (A–D). Expression of *fgfr2* is detected in the in the optic stalk (os), the olfactory placode (op), in rhombomers 1, 4, 6 (R1-6) and in the optic tectum (t) at 24 hpf. These expression domains are still observed at 26 hpf and expression starts in the pharyngeal region (pr). *fgfr2* mRNA is still expressed in the different domains of the brain and in pharyngeal endoderm (pe) until 72 hpf (B, C). Confocal section of double fluorescent *in situ* hybridization for *fgfr2* (red) and *nkx2.3* (green) reveals co-expression in endodermal pouches at 38 hpf (E; yellow arrows). At 48 hpf, *fgfr1a* positive cells co-express *fgfr2* in the pharyngeal endoderm (pe) and in the otic vesicle (ov) (F, yellow). The *sox9a* expression domain (red) in cartilage (cb) surrounds that of *fgfr2* (green) at 72 hpf (G). Scale bar: 150 μm.

corresponds to a slightly more intensely stained cartilage and an abnormal position of the ceratohyals (Fig. 5F). The proportions of each observed phenotype at the indicated conditions are summarized in the form of a table (Fig. 5G).

Two additional morpholinos targeting *fgfr1a* mRNA were tested, one directed against the 5′ UTR region of *fgfr1a* (5′ UTR MOFgfr1a) and one splicing morpholino (sMOFgfr1a). Microinjection resulted in 42% and 47% of type D cartilage, respectively for sMOFgfr1a and 5′ UTR MOFgfr1a (Fig. 5G). Microinjection of a splicing morpholino directed against *fgfr2* mRNA (MOFgfr2) resulted in less severe cartilaginous defects than those injected with MOFgfr1a. Only 16% of Fgfr2 morphants are strongly affected (type D), while 65%
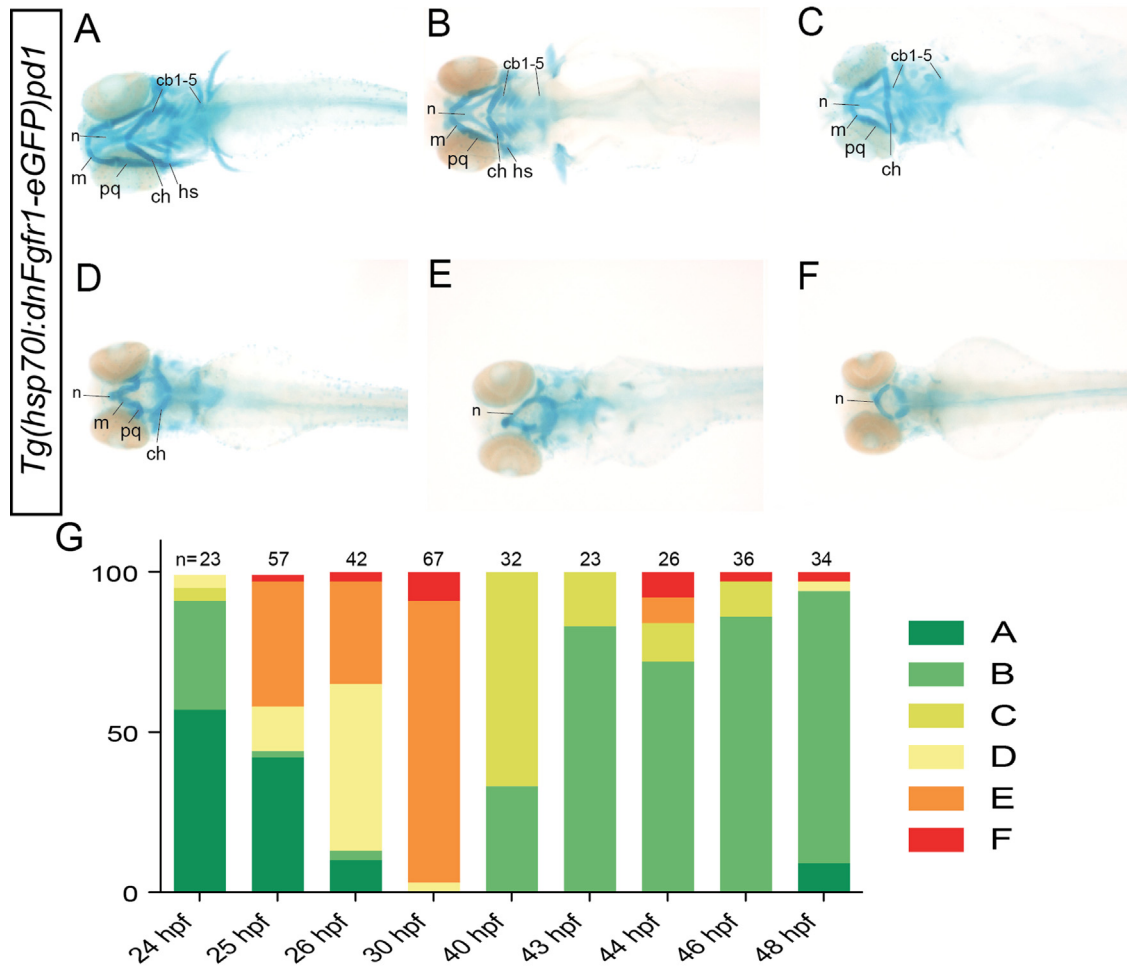
Fig. 3. Inhibition of Fgf signaling beyond 24 hpf perturbs craniofacial cartilage formation. Alcian blue staining at 4 dpf of transgenic *Tg(hsp70l:dnFgfr1-eGFP)pd1* embryos after a heat shock at 37 °C during 30 min starting at the indicated times after fertilization. (A–F) Ventral views, anterior to the left. Six different phenotypes are observed, ranging from (A) wild type like, all cartilaginous structures are present through (B) all structures are present but reduced in size, (C) all structures are present but a strong modification of the ceratohyoid axis and a reduction of the mandible size is observed, (D) strong modifications of the ceratohyoid and the mandible and absence of ceratobranchial arches, (E) remnants of the viscerocranium and defects in the neurocranium to (F) no viscerocranium and strongly affected neurocranium. m: Meckel's cartilage; pq: palatoquadrate; ch: ceratohyoid; hs: hyosymplectic; n: neurocranium; cb1-5: ceratobranchial 1–5. (G) The proportion of strongly affected cartilage (D–F) dramatically increases when heat shock is performed between 26 hpf and 30 hpf, while treatment after 40 hpf causes only weak cartilage defects (B, C).
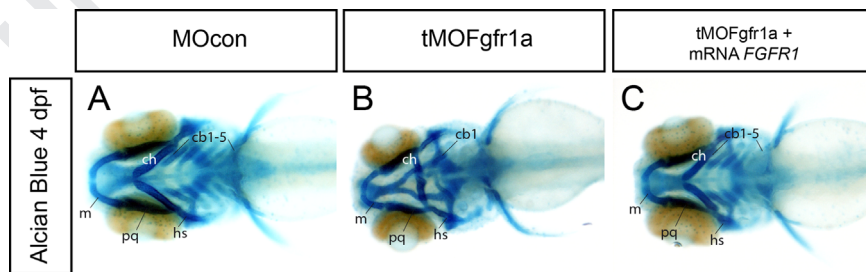

Fig. 4. Knockdown of *fgfr1a* expression generates cartilage defects at 4 dpf. Ventral view, anterior to the left. Wild type and control MO injected embryos display a normal growth of the different pieces of pharyngeal cartilage (A). At this stage, Meckel's cartilage (m), palatoquadrate (pq), ceratohyoid (ch), hyosymplectic (hs) and ceratobranchials (cb1-5) are formed. In tMOFgfr1a morpholino injected embryos, we predominantly observe an absence of the ceratobranchial cartilage, a dorsal modification of the axis of the hyoid and a strong reduction of the mandible (B) (47%). When mRNA for human *FGFR1* is coinjected with tMOFgfr1a, all pharyngeal cartilage pieces are restored (C; 38%).

presented a type C head cartilage (Fig. 5G). Evaluation of MAPK phosphorylation revealed that both tMOFgfr1a and MOFgfr2 injection lead to a significant decrease of Fgf signaling at 30 hpf (Movie S1, Fig. S1E–G). Co-injection of mRNA coding for zebrafish Fgfr2 together with MOFgfr2 resulted in rescue of the severe defects, with larvae presenting normal (type A) or mildly affected (type B) head cartilage. Ectopic expression of either human FGFR1 or zebrafish Fgfr2 alone generated larvae with normal or mildly affected head cartilage (type A, B; Fig. 5) or with slightly hypertrophic cartilage elements (14% and 25%, respectively) (Fig. 5F, G). Co-injection of tMOFgfr1a and MOFgfr2 generated respectively 52% of type C, 38% of type D and 12% of type E cartilage. Efficacy of the splicing morpholinos was verified by RT-PCR on mRNA from 48 hpf morphants (Movie S1, Fig. S1H). Taken together, these results clearly suggest that both Fgfr1a and Fgfr2 are crucial for viscerocranium formation during chondrogenesis.
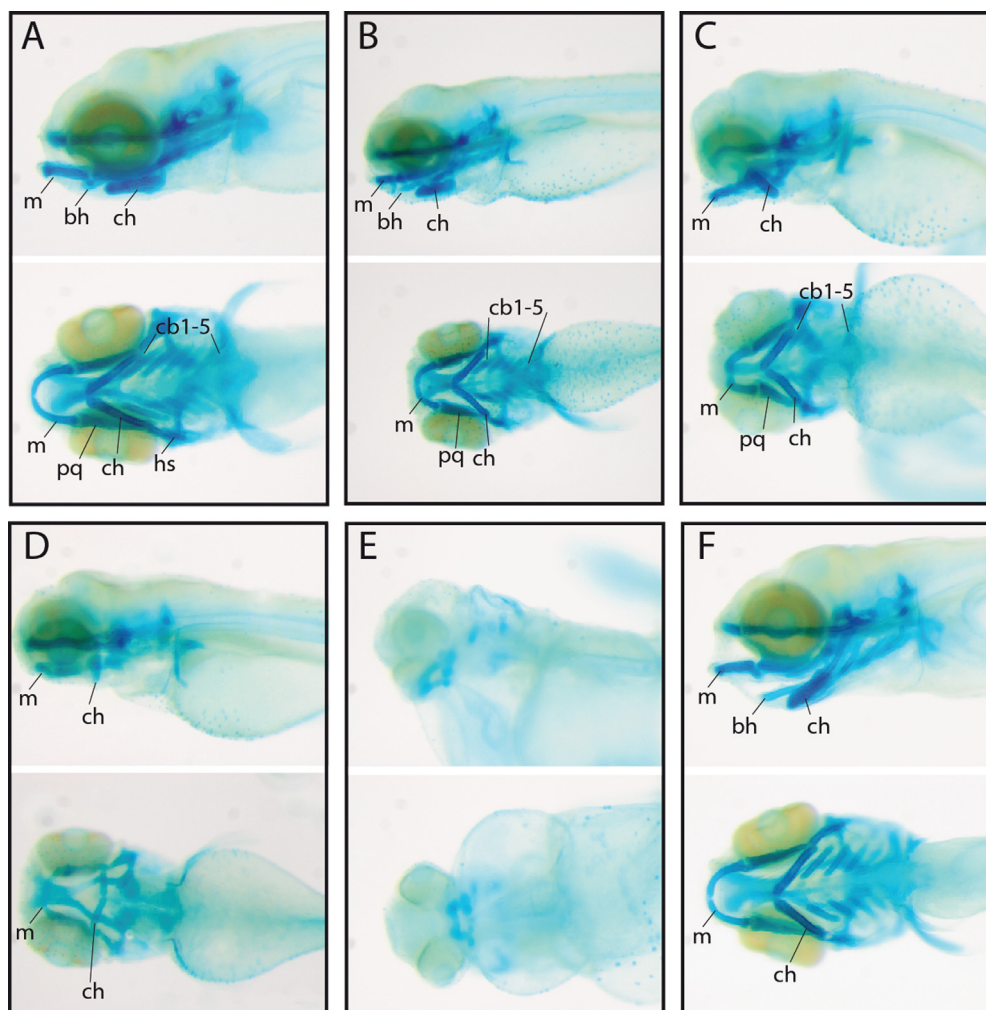
Table 1. Cartilage phenotypes in *fgfr1a* and *fgfr2* morphants.

	n	Cartilage phenotype (%)					
		A	B	C	D	E	F
Uninjected	331	**84**	14	1	1	0	1
MOcon	317	**92**	5	<1	<1	<1	2
tMOFgfr1a	377	5	18	11	**49**	17	0
sMOFgfr1a	125	26	29	1	**42**	2	0
5' UTR MOFgfr1a	296	8	22	8	**47**	15	0
tMOFgfr1a + mRNA *FGFR1*	305	38	**48**	3	8	3	0
mRNA *FGFR1*	186	**58**	25	2	0	1	14
MOFgfr2	156	19	0	**65**	16	0	0
MOFgfr2 + mRNA*fgfr2*	229	44	**48**	4	2	2	0
mRNA *fgfr2*	235	**73**	1	0	1	0	25
tMOFgfr1a + MOFgfr2	275	0	0	**52**	36	12	0
tMOFgfr1a + mRNA*fgfr2*	271	26	**66**	0	8	0	0
tMOFgfr1a + mRNA*runx3*	176	**56**	34	2	0	1	7
tMOFgfr1a+ mRNA *egr1*	173	10	**33**	29	10	18	0
MOFgfr2 + mRNA*runx3*	253	**66**	29	1	1	0	3
MOFgfr2 + mRNA*egr1*	148	11	**76**	4	2	7	0
mRNA *runx3*	239	**89**	7	1	1	0	2
mRNA *egr1*	126	**85**	0	0	0	5	10

Fig. 5. Cranial cartilage structures observed in 4 dpf larvae previously injected with *fgfr1a* and *fgfr2* morpholinos and/or mRNA. At this stage, Meckel's cartilage (m), palatoquadrate (pq), ceratohyoid (ch), hyosymplectic (hs) and ceratobranchials (cb1-5) are formed. Panels A–F illustrate the different cartilage types that were observed in these experiments, lateral and ventral views, anterior to the left. (A) Wild type and control Mo injected embryos display a normal growth of the different pieces of pharyngeal cartilage. (B) mildly affected cartilage. (C) strongly laffected head cartilage with ceratobranchial arches still present, (D) strongly affected cartilage also lacking ceratobranchial arches. (E) only remnants of the neurocranium are observed. (F) embryos displaying a stronger staining of cartilage and an abnormal position of the ceratohyal. (G) table summarizing the proportions of each type of head cartilage pattern observed in the indicated experiments. Column "n" indicates the number of observed individuals for that particular experiment. Bold numbers indicate the highest proportion of cartilage phenotype in each experiment and red numbers concern the increased cartilage phenotype.
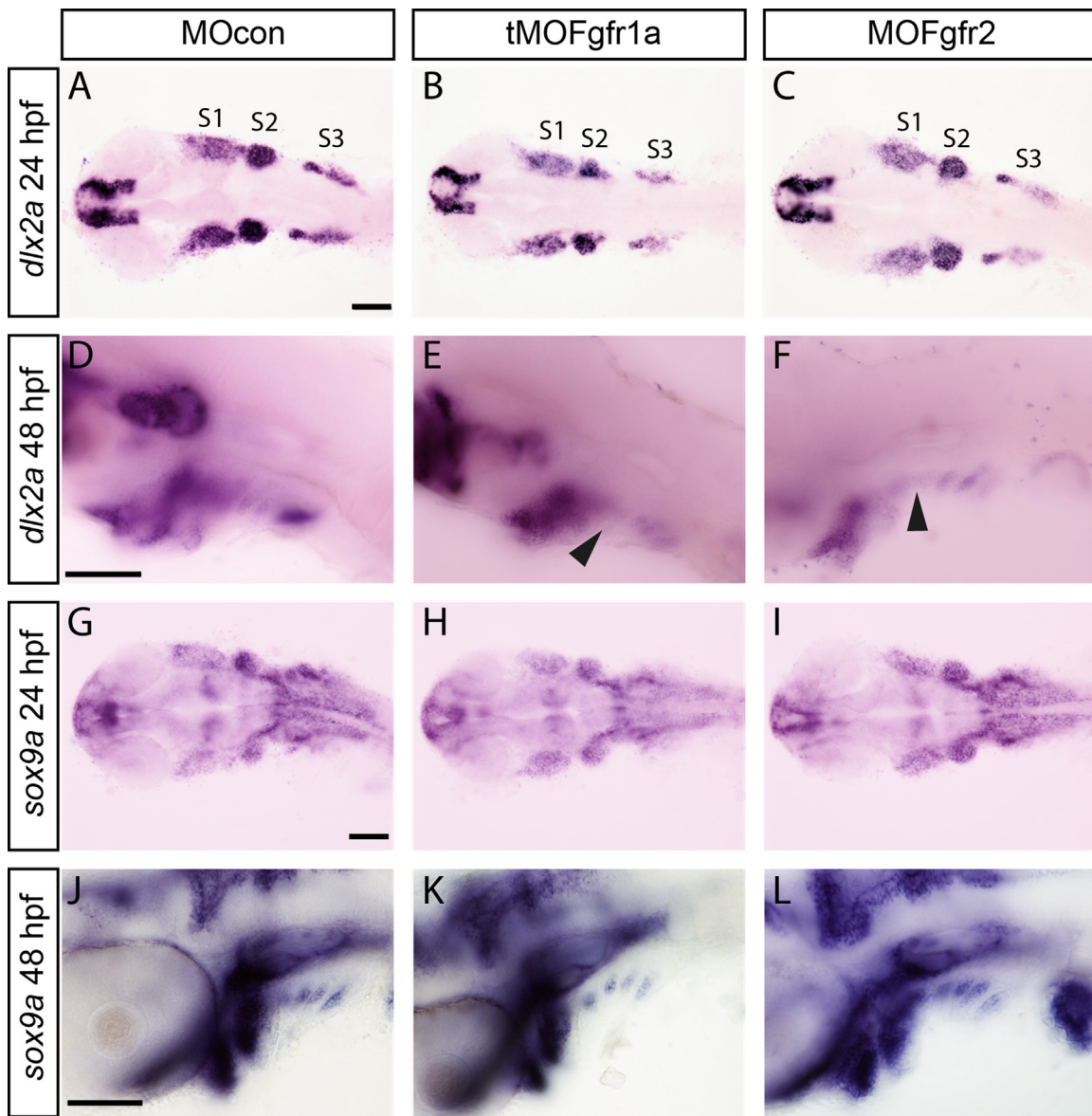
Fig. 6. Fgfr1a and Fgfr2 are not required for *dlx2a* and *sox9a* expression. ISH on morphants with probes for *dlx2a* (A–F) and *sox9a* (G-M) show no difference of the expression pattern of these genes compared to control embryos at 24 hpf (A–C, G–I) and at 48 hpf (D–F, J–L), except for a minor modification of the *dlx2a* expression domain (black arrows; F,G). Anterior is to the left. Ventral views (A–C, G–I) and lateral views (D–F, J–L). Scale bar: 100 μm.

To test whether one receptor can rescue depletion of the other, we co-injected *fgfr2* mRNA into tMOFgfr1a morphants, leading to rescue of the observed defects with a decrease in the proportion of strongly affected larvae (type D, from 49% to 8%; Fig. 5G) and an increase of embryos with only slight modifications of cartilage structure (type B, from 18% to 66%; Fig. 5G).

3.4. Early neural crest cell differentiation does not require Fgfr1a and Fgfr2

To investigate the function of *fgfr1a* and *fgfr2* genes in early differentiation of neural crest cells, we performed ISH on morphants using probes for *dlx2a*, a marker of migrating and post migratory cNCCs (Sperber et al., 2008; Akimenko et al., 1994) and for *sox9a*, a transcription factor involved in chondrocyte maturation (Yan et al., 2005). In all experiments, the expression patterns of *dlx2a* (Fig. 6A–F; Movie S3, Fig. S3) and *sox9a* (Fig. 6G–L; Movie S2, Fig. S2; Movie S3, Fig. S3) remained unaffected both in Fgfr1a and Fgfr2 morphants at 24 and 48 hpf, although a slight decrease

of *dlx2a* expression was observed at 48 hpf in branchial arches 1 and 2 in both *fgfr1a* and *fgfr2* morpholino-injected embryos (Fig. 6D–F). Double fluorescent *in situ* hybridization in control embryos at 24, 30 and 48 hpf revealed that *dlx2a*-expressing cells are intermingled with those expressing *sox9a* in the pharyngeal arches, with patches of cells expressing only one of these factors neighboring domains of cells expressing both mRNAs (Movie S3, Fig. S3 A, D, G). Moreover, the expression and colocalisation domains of *sox9a* and *dlx2a* mRNAs are not affected in *fgfr1a* or *fgfr2* morphants (Movie S3, Fig. S3 A–I) although a slight reduction of their expression domains is observed at 48 hpf. Similarly, expression of GFP in *fli*-GFP transgenic embryos was not affected at 48 hpf after injection of tMOFgfr1a or MOFgfr2, although Fgfr1a knockdown led to perturbations in the branchial arches (Movies S4, Fig. S4). Th.e absence of substantial modifications in *dlx2a*, *sox9a* and *fli1* expression in morphants suggests that migration of neural crest cells and their first steps of differentiation within the endodermal pouches are normal.
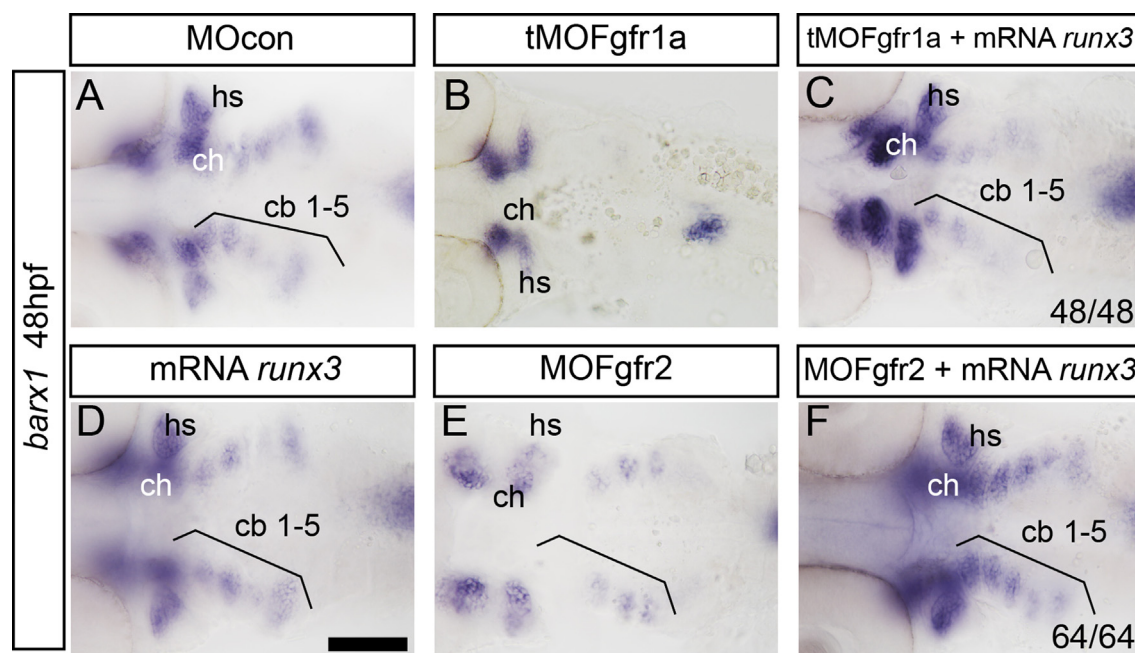
Fig. 7. *barx1* expression is down-regulated in Fgfr1a and Fgfr2 morphants at 48 hpf. In control embryos at 48 hpf, *barx1* transcripts are detected in chondrocytes of the ceratobranchial arches (cb1-5), the ceratohyoid (ch), the hyosymplectic (hs) and in the mandibular zone (A). Depletion of Fgfr1a leads to a dramatic decrease of *barx1* expression in the ceratobranchial chondrocytes (B), while a more modest decrease is observed in Fgfr2 morphants in the pharyngeal region (E) compared to control. *runx3* mRNA injection does not affect the *barx1* expression pattern (D). Co-injection of *runx3* mRNA with tMOFgfr1a or MOFgfr2 restores wild type expression of *barx1* (C, F) in 100% of morphants. Ventral views, anterior to left. Scale bar: 100 μm.
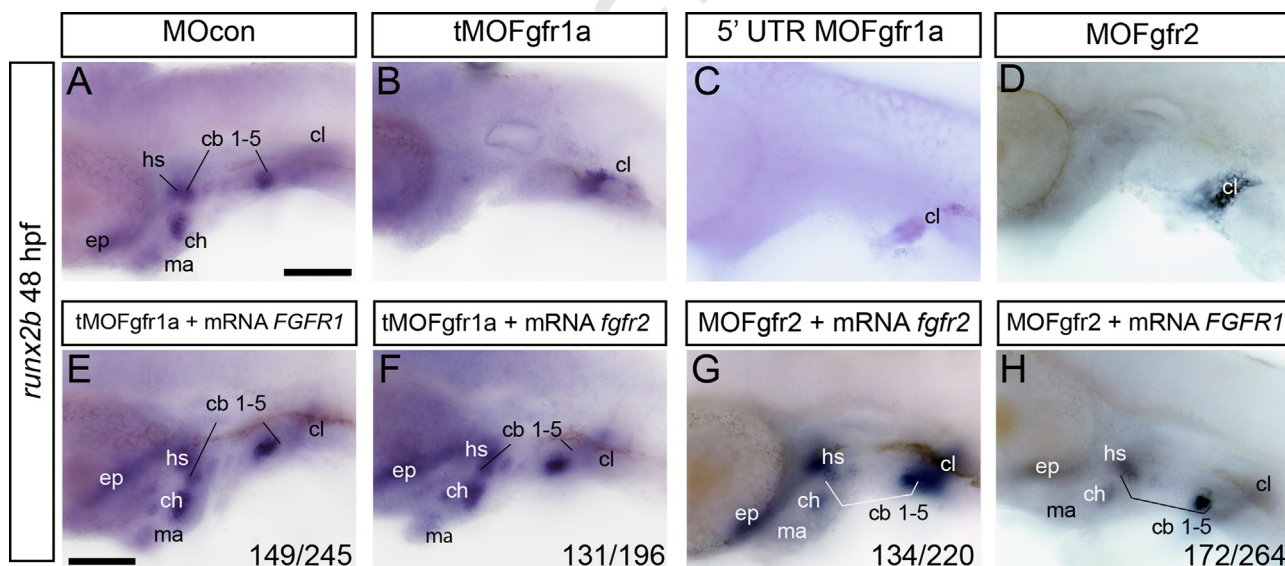

Fig. 8. Transcription of the *runx2b* gene is decreased in Fgfr1a and Fgfr2 morphants. Lateral views of *in situ* hybridizations, anterior to the left. At 48 hpf, *runx2b* expression in absence of *fgfr1a* is observed only in the cleithrum (cl) (B,C), while in control embryos *runx2b* transcripts are detected in the mandible (ma), in the ceratohyoid (ch), in the hyosymplectic (hs), in ceratobranchials (cb1-5) and in the ethmoid plate (ep) (A,F). Ectopic expression of *FGFR1* mRNA in morphants for Fgfr1a restores *runx2b* expression in the pharyngeal cartilages (D, 61% *n*=149/245), similar to co-injection of tMOFgfr1a and *fgfr2* mRNA (E, 67% *n*=131/196). In Fgfr2 morphants, *runx2b* expression persists only in the cleithrum (G,H). Co-injection of *FGFR1* mRNA and MOFgfr2 restores wild type *runx2b* expression in 61% (*n*=134/220) of the embryos (I) and 65% (*n*=172/264) of embryos have a wild type *runx2b* expression pattern when morpholino against *fgfr2* is co injected with *fgfr2* mRNA (J). Scale bar: 100 μm.

3.5. Fgfr1a and Fgfr2 are required for condensation and late differentiation of chondrocytes

Barx1 is a transcription factor involved in condensation of cranial neural crest cells whose expression was shown to be controlled by Fgf signaling (Sperber and Dawid, 2008). Moreover, *barx1* expression is essential for *runx2b* expression, a transcription factor absolutely required for chondrocyte maturation (Flores et al., 2006; Flores et al., 2004) in the pharyngeal region. At 48 hpf, *barx1* mRNA is detected in chondrocytes of the ceratobranchial arches, the hyosymplectic and the ceratohyal in control embryos (Fig. 7A) (Sperber and Dawid, 2008). At this stage, *fgfr1a* or *fgfr2* knock-down caused a reduction of *barx1* expression, to different extents (Fig. 7B, E).

At 48 hpf, *runx2b* mRNAs are observed in the mandible, the hyoid, the ceratobranchial arches, the ethmoid plate and in the cleithrum (Fig. 8A). In Fgfr1a or Fgfr2 morphants, all *runx2b* expression domains are absent in the pharyngeal region except
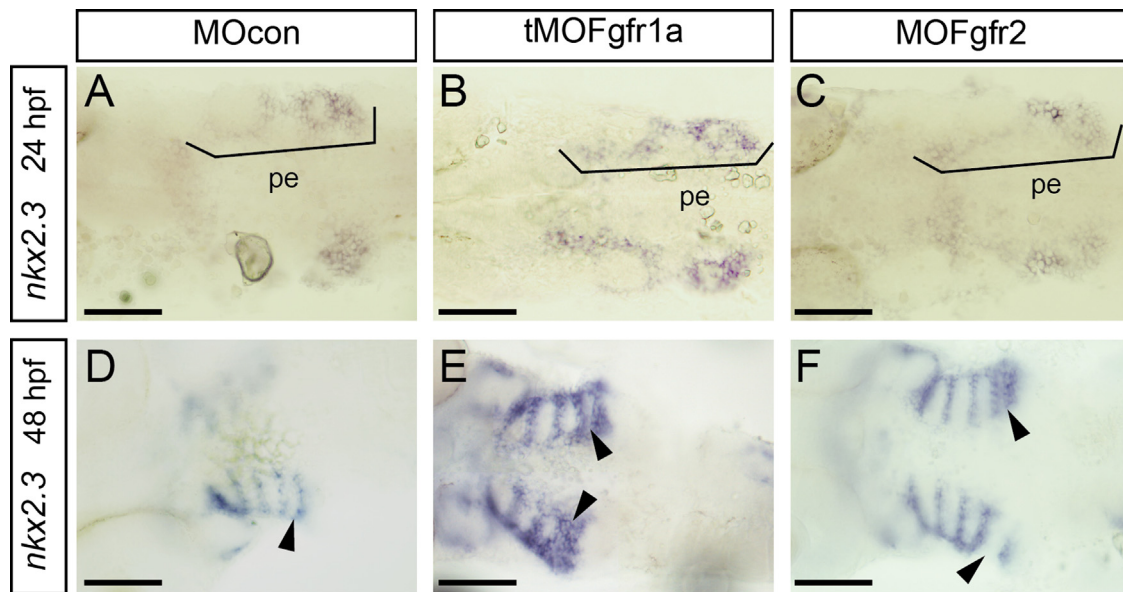
Fig. 9. Endodermal expression of *nkx2.3* is maintained in the pharyngeal region upon Fgfr1a and Fgfr2 knock-down. In both Fgfr1a and Fgfr2 morphants, *nkx2.3* expression is still observed in the pharyngeal region at 24 hpf and 48 hpf. However, *nkx2.3* patterning is modified in the ceratobranchial 5 region (E, F; arrows) at 48 hpf. Ventral views, anterior to the left. pe: pharyngeal endoderm. Scale bar: 100 μm.

for its expression in the cleithrum (Fig. 8B–D). Rescue experiments reveal that co-injection of tMOFgfr1a with human *FGFR1* mRNA or zebrafish *fgfr2* restores wild type *runx2b* expression in 61% (*n*=149/245) and 67% (*n*=131/196) of the larvae, respectively (Fig. 8E, F). Similarly, MOFgfr2-injected embryos recover expression of *runx2b* in the pharyngeal region when *FGFR1* mRNA or mRNA *fgfr2* is co-injected, respectively in 61% (*n*=134/220) and 65% (*n*=172/264) of injected embryos (Fig. 8G, H). These data suggest that the two receptors are involved in condensation and late maturation of chondrocytes.

3.6. Fgfr1a and Fgfr2 are not essential for formation of the endodermal pouches

To determine the function of the two receptors in endodermal pouch formation, we performed *in situ* hybridization with the endodermal marker *nkx2.3* (Lee et al., 1996) on both morphants. At 24 and 48 hpf and in comparison with control embryos, loss of function of *fgfr1a* or *fgfr2* does not affect *nkx2.3* expression, only a modification of the endodermal pouch patterning was observed in the ceratobranchial 5 (cb5) region (arrows; Fig. 9E, F) at 48 hpf. We also observed that Fgfr1a depletion does not affect *fgfr2* expression and conversely Fgfr2 depletion does not affect *fgfr1a* expression in the pharyngeal endoderm at 48 hpf (Fig. 10). Similarly, injection of both morpholinos into sox17-GFP (Sakaguchi et al., 2006) transgenic embryos revealed that expression of this endodermal marker is maintained, albeit again displaying an aberrant patterning of the cb5 pouches at 48 hpf (Moive S5, Fig. S5 B, C).

These results suggest that both Fgfr1a and Fgfr2 are not required for formation of the pharyngeal endoderm, but contribute to its correct shaping at 48 hpf.

3.7. Fgfr1a and Fgfr2 activate the Runx3–Egr1–Sox9b–fsta cascade in pharyngeal endoderm

Recently, a regulatory cascade was described in zebrafish pharyngeal endoderm involving the transcription factors Runx3–Egr1–Sox9b (Dalcq et al., in press) that inhibits expression of Follistatin A, a BMP inhibitor. This down-regulation allows the full activity of BMP signaling required for expression of *runx2b* in

cartilage mesenchyme. We investigated the effect of Fgfr1a or Fgfr2 depletion on this cascade.

In control embryos, *runx3* expression was observed at 48 hpf in pharyngeal endoderm, the cleithrum and the trigeminal ganglion (Fig. 11A, C), as expected (Flores et al., 2006). Knockdown of each receptor decreases *runx3* expression in the pharyngeal endoderm (Fig. 11B, D), while its expression in the cleithrum and in the trigeminal ganglia is still present. This effect is specific, as co-injection of MOFgfr2 with *fgfr2* or human *FGFR1* mRNA caused respectively 87% (*n*=47/54) or 85% (*n*=59/70) of larvae to recover *runx3* expression in the pharyngeal endoderm.

At 72 hpf, *egr1* expression can be detected in oral epithelium, in the brain and in the pharyngeal endoderm of control embryos (Fig. 11G, I). Fgfr1a and Fgfr2 morphants showed an absence of *egr1* expression in the pharyngeal endoderm whereas the other expression domains remain unchanged (Fig. 11H, J).

At 48 hpf, *sox9b* mRNA is localized in pharyngeal endoderm, in the hindbrain, in the tectum and in the pectoral fin bud in control embryos (Fig. 11K, M) (Yan et al., 2005). *In situ* hybridizations indicate that Fgfr1a or Fgfr2 knock down leads to an absence of *sox9b* expression in the endodermal pouches (Fig. 11 L,N) and a decrease in the mandibular and hyoid region, whereas expression in the hindbrain is maintained.

Sox9b was shown to repress expression of the secreted BMP inhibitor follistatin A in pharyngeal endoderm, thereby allowing correct BMP signaling to the developing chondrocytes (Dalcq et al., in press). In control embryos, we observed weak *fsta* expression in the pharyngeal region at 48 hpf (Fig. 11O, Q), while *fsta* transcription was strongly upregulated when tMOFgfr1a or MOFgfr2 were injected into one-cell stage embryos (Fig. 11P, R).

To further support the involvement of Fgfr1a and Fgfr2 receptors in activation of the endodermal regulatory cascade, we tested whether ectopic expression of Egr1 or Runx3 would be able to rescue the cartilage defects in Fgfr morphants. Injection of either *egr1* or *runx3* mRNA together with tMOFgfr1a or MOFgfr2 resulted in a drastic decrease of the severe phenotypes observed in Fgfr morphants (table in Fig. 5G). In 48 hpf embryos, co-injection of *runx3* mRNA with tMOFgfr1a resulted in partial (43%, *n*=57/133) or near complete (52%, *n*=69/133) rescue of *runx2b* expression (Fig. 12A–D). Ectopic Runx3 expression partially (33%, *n*=38/115)
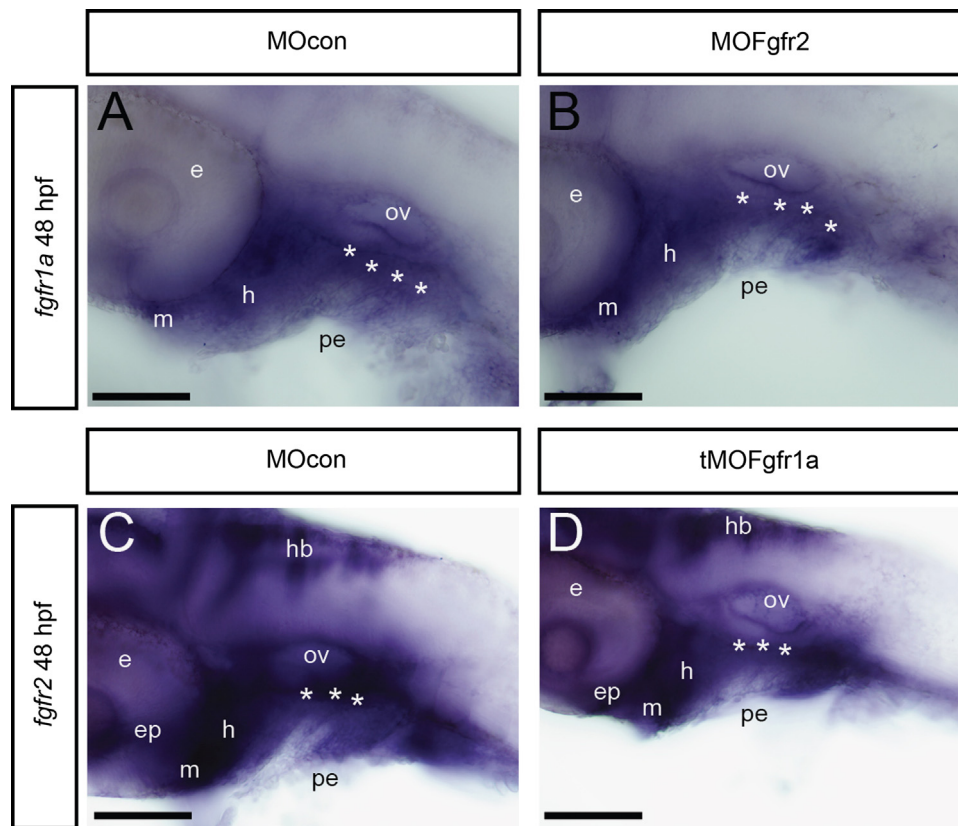
Fig. 10. No mutual regulation between *fgfr1a* and *fgfr2* in the pharyngeal region. Lateral view of *in situ* hybridization, anterior is to the left. At 48 hpf, Fgfr2 knock down does not affect *fgfr1a* expression in the pharyngeal endoderm (pe), mandible region (m) and hyoid region (h) (B) compared to control embryos (A). Similarly, *fgfr2* expression is still observed at 48 hpf (D) in pharyngeal endoderm (pe), mandibular and hyoid region (m, h), hindbrain (hb) and ethmoid placode (ep) in control and Fgfr1a morphants embryos. Scale bar: 100 μm.

or completely (62%, $n=71/115$) rescued Fgfr2 knockdown, while injection of *runx3* mRNA alone had no effect (Fig. 12E–H). Similarly, injection of *runx3* mRNA rescued the loss of *barx1* expression caused by tMOFgfr1a (100% rescue, $n=48/48$) or MOFgfr2 (100% rescue, $n=64/64$)(Fig. 7C, F).

These results show that in pharyngeal endoderm, both Fgfr1a and Fgfr2 control the endodermal cascade involved in chondrogenesis.

4. Discussion

4.1. The receptors Fgfr1a and Fgfr2 are required for late differentiation of pharyngeal chondrocytes

The development of head cartilage, deriving from cranial neural crest cells and forming the matrix for subsequent endochondral bone formation, depends on a complex and precisely controlled interplay between different extracellular signaling pathways. Among these, Fgf signaling has been extensively studied in zebrafish. Fgf3 and Fgf8 ligands produced in the hindbrain and lateral mesoderm are required during early segmentation stages for correct organization of the endodermal pouches (Crump et al., 2004). Later, Fgf signaling is required in cNCCs for their conversion into the ectomesenchymal lineage, characterized by *dlx2a* expression, after migration into the endodermal pouches (Blentic et al., 2008). Endodermal expression of *fgf3* is required for *dlx2a* expression in post migratory cNCCs and their survival in the posterior arches (David et al., 2002; Nissen et al., 2003), while loss of function of both *fgf3* and *fgf8* affect differentiation and survival of cNCCs as well as *dlx2a* expression in all the arches (Crump et al., 2004; Walshe and Mason, 2003). Thus, Fgf signaling acts during

segmentation stages before 24 hpf on pharyngeal cartilage formation through cell-autonomous mechanisms within cNCC-derived chondrocyte precursors and indirectly through patterning of the pharyngeal endoderm.

In this study, we examined the role of Fgf signaling during craniofacial cartilage formation using the transgenic line *Tg* (*hsp70l:dnfgfr1-EGFP*)*pd1* which allows controlled expression of a dominant negative Fgf receptor mutant (Ota et al., 2010). We show an additional function for Fgf signaling at later stages in chondrogenesis, which is most effective after 30 hpf compared to earlier (24–26 hpf) or later (beyond 40 hpf) stages. At this stage, conversion of cNCCs to ectomesenchyme is finished and the first steps of chondrocyte differentiation, such as *sox9a* expression, are initiated.

As the dominant negative receptor blocks signaling by interacting with endogenous receptors in the cells where it is expressed, we decided to study the role of Fgfr1a and Fgfr2 receptors by antisense morpholino injection, as both were previously shown to be expressed in the pharyngeal region at 24 hpf (Tonou-Fujimori et al., 2002; Ota et al., 2010). Depletion of each Fgfr1a or Fgfr2 leads to severe defects in cranial cartilage formation, similar to those observed upon Fgf inhibition after 24 hpf. Efficacy of the splicing morpholinos was verified by RT-PCR, while unspecific effects due to morpholino injection were excluded by co-injecting a morpholino against p53 to block unspecific apoptosis (Robu et al., 2007) in all experiments. Results obtained in the presence of MOp53 were similar to those obtained without co-injection (data not shown). In addition, we tested three different morpholinos directed against *fgfr1a* with similar results and we show that the defects caused by depletion of each receptor are rescued by ectopic expression of exogenous receptor. Furthermore,
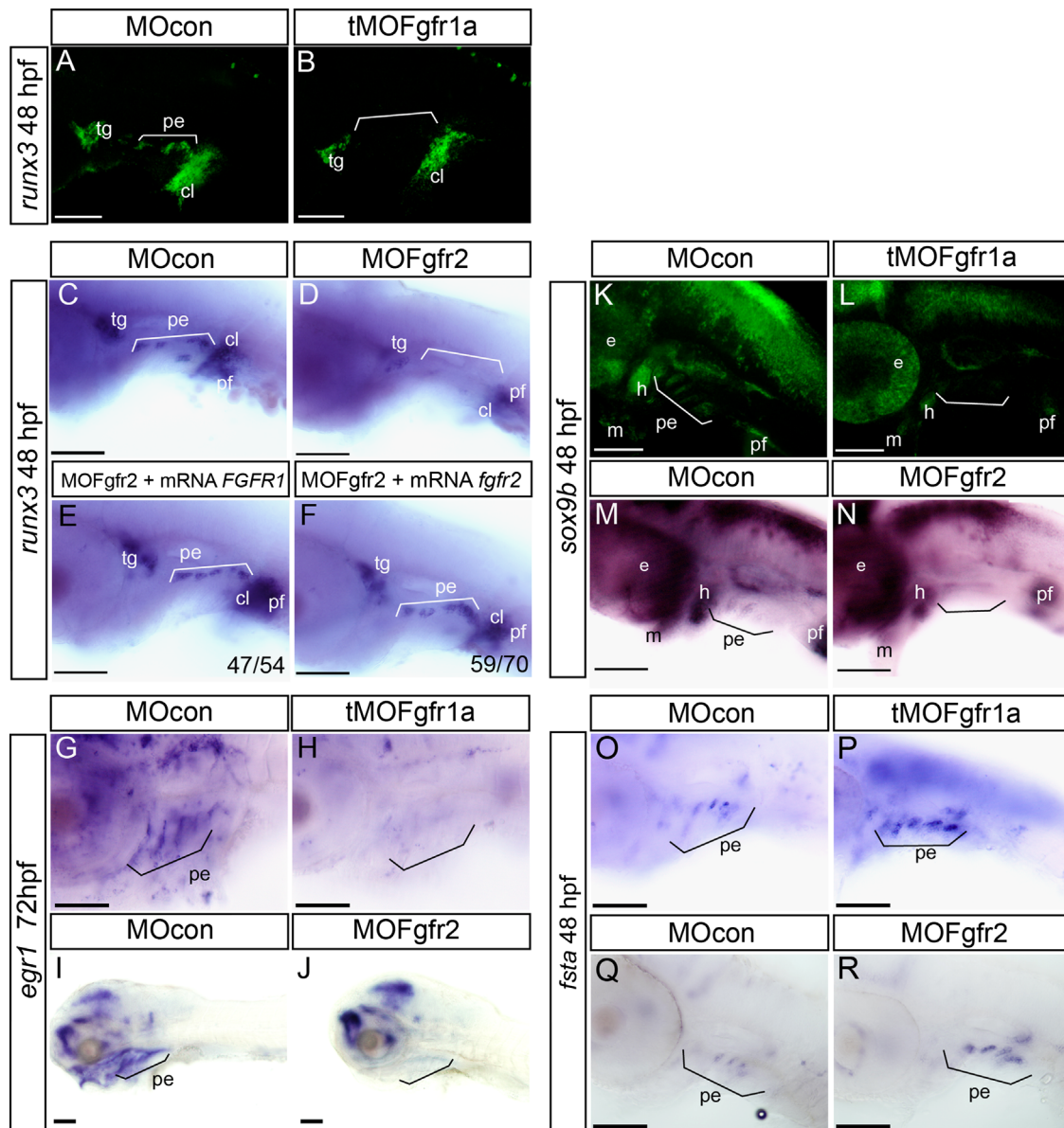
Fig. 11. Fgfr1a or Fgfr2 knockdown leads to decreased expression of *runx3*, *egr1* and *sox9b* in the pharyngeal endoderm. Lateral view, anterior to the left. At 48 hpf, *runx3* expression in the pharyngeal endoderm (pe) is absent in Fgfr1a and Fgfr2 morphants, whereas its expression is still observed in the cleithrum (cl), the pectoral fin (pf) and in the trigeminal ganglia (tg) (B, D). Co-injection of *FGFR1* mRNA with morpholino against Fgfr2 restores *runx3* expression in pharyngeal endoderm at 48 hpf (E, n=59/70). Similarly, *runx3* mRNA expression is restored when *fgfr2* mRNA is co-injected with MOFgfr2 (F, n=47/54). At 72 hpf in both Fgfr1a and Fgfr2 morphants, *egr1* expression is absent in the pharyngeal endoderm (pe), while its expression is still present in the different parts of the brain (H,J) compared to control embryos (G, I). Compared to control embryos (K, M), the endodermal marker *sox9b* is absent in the pharyngeal endoderm of the ceratobranchial region at 48 hpf when Fgfr1a or Fgfr2 are downregulated (L, N). Moreover, *sox9b* expression is reduced in the mandibular (m) and hyoid region (h) in both receptor morphants (L, N). At 48 hpf, *fsta* expression in the pharyngeal endoderm is upregulated in *fgfr1a* and *fgfr2* morphants (P, R) compared to injected control embryos (O, Q). Scale bar: 100 μm.

ectopic expression of the receptors alone led to either no defect or an increase in cartilage formation.

When we investigated the effect of receptor depletion on chondrocyte differentiation, we observed that expression of *dlx2a* and of *sox9a* is maintained at 24 and 48 hpf. By double fluorescent *in situ* hybridization at 24, 30 and 48 hpf, we observed three types of domains within the ectomesenchymal condensations: one domain mostly consisting of cells expressing both *dlx2a* and *sox9a*, the other two formed of cells expressing either *dlx2a* or *sox9a*. One possible explanation for this observation would be that cells expressing first *dlx2a* only subsequently differentiate into cells expressing both factors and finally into *sox9a*-only expressing cells. Importantly, we did not observe a substantial modification of this combined expression pattern in Fgf receptor morphants, suggesting an absence of effect on developmental timing.

In contrast, expression of the late chondrocyte marker *runx2b* was completely abolished in the pharyngeal arches, indicating that cNCC formation, migration and early differentiation are not affected, while late maturation is absent.

In addition, we observe a decreased expression of *barx1* in the pharyngeal arches of both Fgfr1a and Fgfr2 morphants. In mouse, *Barx1* is expressed in cranio-facial ectomesenchyme and the stomach (Tissier-Seta et al., 1995), it is required for differentiation of the stomach epithelium by controlling expression of Wnt signaling inhibitors and for spleen morphogenesis (Woo et al., 2011). In zebrafish, *barx1* expression was observed in a subset of cNCC at 19 hpf, in the three streams of cranial neural crest at 24 hpf and in developing ectomesenchyme at later stages (Sperber and Dawid, 2008). Its expression was abolished in the presence of the Fgf inhibitor SU5402. Morphants for Barx1 displayed a
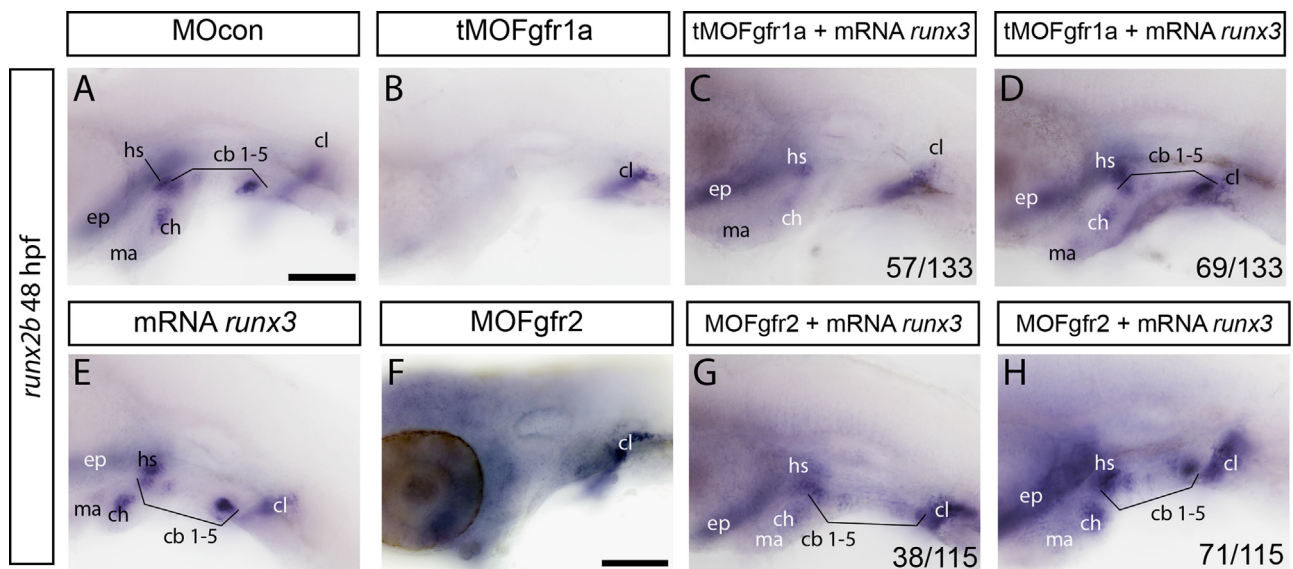
Fig. 12. Co-injection of *runx3* mRNA rescues the defects in tMOFgfr1 and MOFgfr2 morphants. Lateral views of *in situ* hybridizations, anterior to the left. At 48 hpf, *runx2b* expression is detected in the mandible (ma), in the ceratohyoid (ch), in the hyosympletic (hs), in ceratobranchials (cb1-5) and in the ethmoid plate (ep) (A, F) in control embryos, while it is only observed in the cleithrum (cl) in Fgfr1a or Fgfr2 morphants (B, E). Ectopic expression of *runx3* mRNA in Fgfr1a morphants restores expression of *runx2b* in the pharyngeal cartilages partially in 43% ($n=57/133$) of embryos (C) and completely in 52% ($n=69/133$) of injected embryos (D). Co-injection of *runx3* mRNA and MOFgfr2 restores wild type *runx2b* expression in 62% ($n=71/115$) of embryos (G), while 33% ($n=38/115$) of embryos present a decreased expression of *runx2b* (F). Injection of *runx3* mRNA alone does not affect *runx2b* expression in injected embryos (H). Scale bar: 100 μm.

deficiency in prechondrocyte aggregation and various defects in formation of the different pharyngeal cartilage elements. Expression of *dlx2a* and *sox9a* was maintained while *runx2b* expression was decreased. Barx1 was also shown to promote cartilage fate *versus* joints formation in the head (Nichols et al., 2013). Together with these observations, our results suggest that Barx1 is part of a regulatory cascade in developing chondrocytes required for expression of runx2b and subsequent maturation.

4.2. Fgfr1a and Fgfr2 control the function of pharyngeal endoderm in head cartilage formation

At this point, it was important to determine the precise tissues that express these Fgf receptors at the stages beyond 24 hpf. We show that both Fgfr1a and Fgfr2 receptors are expressed in pharyngeal endoderm by double fluorescent *in situ* hybridization revealing their coexpression with the endodermal marker *nkx2.3*, while their expression domains are clearly distinct from those of cNCC markers such as *dlx2a* or *sox9a*. We further show that *fgfr1a* and *fgfr2* expression largely overlaps in pharyngeal endoderm at 48 hpf. This is consistent with the previously described expression for *fgfr1a* in the pharyngeal arches (Ota et al., 2010) and *fgfr2* in axial mesoderm and endoderm at 24 hpf (Tonou-Fujimori et al., 2002). In our experiments, *fgfr2* mRNA was weakly detected in the pharyngeal region at 24 hpf, but clearly observed at 26 hpf, suggesting that its endodermal expression starts around this stage. With the observed timing of the requirement for Fgf signaling around 30 hpf, this observation could explain the somewhat weaker effects observed upon Fgfr2 depletion. Earlier requirement for Fgf signaling in cNCCs during segmentation (Blentic et al., 2008) suggests the presence of an Fgf receptor at this stage in cNCCs, however the exact nature of this receptor was not determined.

Our loss of function studies reveal that both receptors act on the function of pharyngeal endoderm during chondrogenesis. Formation and initial patterning of pharyngeal pouches is not affected, as shown by the intact expression patterns of *nkx2.3* and *sox17*. Only a slight defect is observed at 48 hpf in segmentation of the most posterior pouch, which might arise as a secondary effect

due to the defects in cNCC differentiation. In contrast, expression of later markers of endodermal pouches, such as *runx3*, *egr1* and *sox9b* is severely reduced, indicating that the function of the mature endodermal pouches is abolished. Expression of the three transcription factors Runx3, Egr1 and Sox9b was recently shown to be required in pharyngeal endoderm to reduce expression of *fsta*, coding for the BMP inhibitor follistatin A (Dalcq et al., in press). Consistent with this model, we observed a clear increase of *fsta* expression in Fgfr1a and Fgfr2 morphants. Furthermore, the defects observed in our receptor morphants could be rescued by expression of exogenous Runx3 or Egr1, indicating that the loss of this endodermal regulatory cascade is the major cause for cartilage defects in Fgfr1a or Fgfr2 morphants. Taken together, these observations suggest that the two Fgf receptors are required to initiate the regulatory cascade in pharyngeal endoderm that controls expression of *fsta*, and thus allows correct BMP signaling to the cNCC.

The various Fgf ligands bind to the different receptors with specific affinities and further variation is brought about by the presence of different splicing isoforms for Fgfr1, 2 and 3 (Zhang et al., 2006; Ornitz et al., 1996). Using the human FGFR isoforms, it appears that the two major Fgfs involved in cartilage formation, Fgf3 and Fgf8 are able to bind to at least one isoform of each receptor 1 or 2. The fact that loss of function of each Fgfr1a or Fgfr2 results in cartilage defects points at a non-redundant, specific function for each receptor, which could be brought about by specificity for a particular ligand or specificity in downstream signaling for each receptor. Our results showing that the defects caused by lack of one receptor can be rescued by expression of the other argue against such specificity. We also show that knockdown of one receptor does not affect expression of the other. Although we cannot completely rule out rescue of specific functions of one receptor by exogenous over expression of the other, we favor the explanation of a requirement for a precise amount of receptors to ensure activation of the regulatory cascade. Further support for this interpretation comes from the similarity of the defects observed upon knockdown of each receptor.

Considering the importance of Fgf signaling for the entire development (Itoh and Ornitz, 2011), specifically during segmentation, for
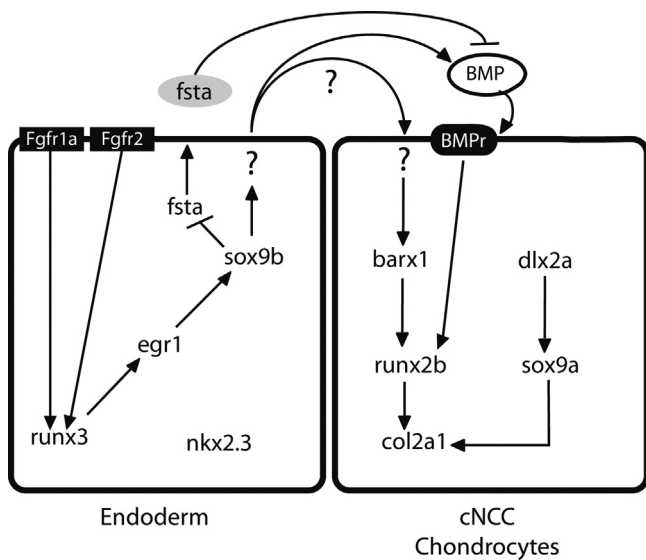
Fig. 13. Fgfr1a and Fgfr2 activate a regulatory cascade required to modulate Bmp-signaling during cranial cartilage development in zebrafish. Signaling model describing the regulatory cascades in pharyngeal endoderm and cNCCs. Fgf signaling through Fgfr1a and Fgfr2 present in pharyngeal endoderm initiate a regulatory cascade composed of the three transcription factors Runx3, Egr1 and Sox9b, which down-regulates *fsta* expression coding for a Bmp antagonist. This down-regulation allows Bmp ligands to bind to their receptor and induce *runx2b* expression in cranial neural crest cells (cNCC).

formation of the pharyngeal arches (Blentic et al., 2008; Crump et al., 2004), it seems surprising that the effects of *fgfr1a* or *fgfr2* knockdown are not more severe. Indeed, the general morphology of the morphants was not much affected, brain segmentation was normal, patterning of the pharyngeal endoderm was close to normal and the first markers for chondrocyte differentiation are present. This is in sharp contrast to the defects observed upon complete Fgf inhibition during segmentation (Crump et al., 2004). Assuming that knockdown of the receptors is probably not complete in our experiments, these observations indicate that the requirement for Fgfr1a and Fgfr2 during these early stages is less stringent and/or that their absence is more efficiently compensated by other members of the Fgfr family, such as Fgfr3.

In conclusion (Fig. 13), we show that Fgf receptors Fgfr1a and Fgfr2 are expressed in zebrafish endodermal pouches beyond 24 hpf, where they are required to ensure activation of a regulatory cascade in pharyngeal endoderm. This cascade reduces expression of the BMP antagonist *fsta*, thereby allowing full activity of BMP signaling in the pharyngeal region to induce chondrocyte maturation in head cartilage.

Acknowledgments

References

Akimenko, M.A., Ekker, M., Wegner, J., Lin, W., Westerfield, M., 1994. Combinatorial expression of three zebrafish genes related to distal-less: part of a homeobox gene code for the head. Journal of Neuroscience 14, 3475–3486.

Alexander, C., Zuniga, E., Blitz, I.L., Wada, N., Le Pabic, P., Javidan, Y., Zhang, T., Cho, K.W., Crump, J.G., Schilling, T.F., 2011. Combinatorial roles for BMPs and Endothelin 1 in patterning the dorsal-ventral axis of the craniofacial skeleton. Development 138, 5135–5146.

Alexander, J., Rothenberg, M., Henry, G.L., Stainier, D.Y., 1999. Casanova plays an early and essential role in endoderm formation in zebrafish. Developmental Biology 215, 343–357.

Baldridge, D., Shchelochkov, O., Kelley, B., Lee, B., 2010. Signaling pathways in human skeletal dysplasias. Annual Review of Genomics and Human Genetics 11, 189–217.

Barrallo-Gimeno, A., Holzschuh, J., Driever, W., Knapik, E.W., 2004. Neural crest survival and differentiation in zebrafish depends on mont blanc/tfap2a gene function. Development 131, 1463–1477.

Blentic, A., Tandon, P., Payton, S., Walshe, J., Carney, T., Kelsh, R.N., Mason, I., Graham, A., 2008. The emergence of ectomesenchyme. Developmental Dynamics 237, 592–601.

Close, R., Toro, S., Martial, J.A., Muller, M, 2002. Expression of the zinc finger Egr1 gene during zebrafish embryonic development. Mechanisms of Development 118, 269–272.

Crump, J.G., Maves, L., Lawson, N.D., Weinstein, B.M., Kimmel, C.B., 2004. An essential role for Fgfs in endodermal pouch formation influences later craniofacial skeletal patterning. Development 131, 5703–5716.

Dalcq, J., Pasque, V., Ghaye, A., Larbuisson, A., Motte, P., Martial, J.A., Muller, M, 2013. Runx3, Egr1 and Sox9b form a regulatory cascade required to modulate BMP-signaling during cranial cartilage development in zebrafish. PLOS One. (in press).

David, N.B., Saint-Etienne, L., Tsang, M., Schilling, T.F., Rosa, F.M., 2002. Requirement for endoderm and FGF3 in ventral head skeleton formation. Development 129, 4457–4468.

Flores, M.V., Lam, E.Y., Crosier, K.E., Crosier, P.S., 2008. Osteogenic transcription factor Runx2 is a maternal determinant of dorsoventral patterning in zebrafish. Nature Cell Biology 10, 346–352.

Flores, M.V., Lam, E.Y., Crosier, P., Crosier, K, 2006. A hierarchy of Runx transcription factors modulate the onset of chondrogenesis in craniofacial endochondral bones in zebrafish. Developmental Dynamics 235, 3166–3176.

Flores, M.V., Tsang, V.W., Hu, W., Kalev-Zylinska, M., Postlethwait, J., Crosier, P., Crosier, K., Fisher, S., 2004. Duplicate zebrafish runx2 orthologues are expressed in developing skeletal elements. Gene Expression Patterns 4, 573–581.

Goldring, M.B., Tsuchimochi, K., Ijiri, K., 2006. The control of chondrogenesis. Journal of Cellular Biochemistry 97, 33–44.

Hall, C., Flores, M.V., Murison, G., Crosier, K., Crosier, P., 2006. An essential role for zebrafish Fgfrl1 during gill cartilage development. Mechanisms of Development 123, 925–940.

Hung, I.H., Yu, K., Lavine, K.J., Ornitz, D.M., 2007. FGF9 regulates early hypertrophic chondrocyte differentiation and skeletal vascularization in the developing stylopod. Developmental Biology 307, 300–313.

Itoh, N., 2007. The Fgf families in humans, mice, and zebrafish: their evolutional processes and roles in development, metabolism, and disease. Biological and Pharmaceutical Bulletin 30, 1819–1825.

Itoh, N., Ornitz, D.M., 2008. Functional evolutionary history of the mouse Fgf gene family. Developmental Dynamics 237, 18–27.

Itoh, N., Ornitz, D.M., 2011. Fibroblast growth factors: from molecular evolution to roles in development, metabolism and disease. Journal of Biochemistry 149, 121–130.

Kimmel, C.B., Ballard, W.W., Kimmel, S.R., Ullmann, B., Schilling, T.F., 1995. Stages of embryonic development of the zebrafish. Developmental Dynamics 203, 253–310.

Kluver, N., Kondo, M., Herpin, A., Mitani, H., Schartl, M., 2005. Divergent expression patterns of Sox9 duplicates in teleosts indicate a lineage specific subfunctionalization. Development Genes and Evolution 215, 297–305.

Knight, R.D., Schilling, T.F., 2006. Cranial neural crest and development of the head skeleton. Advances in Experimental Medicine and Biology 589, 120–133.

Lee, K.H., Xu, Q., Breitbart, R.E., 1996. A new tinman-related gene, nkx2.7, anticipates the expression of nkx2.5 and nkx2.3 in zebrafish heart and pharyngeal endoderm. Developmental Biology 180, 722–731.

Lee, Y., Grill, S., Sanchez, A., Murphy-Ryan, M., Poss, K.D., 2005. Fgf signaling instructs position-dependent growth rate during zebrafish fin regeneration. Development 132, 5173–5183.

Nakayama, Y., Miyake, A., Nakagawa, Y., Mido, T., Yoshikawa, M., Konishi, M., Itoh, N., 2008. Fgf19 is required for zebrafish lens and retina development. Developmental Biology 313, 752–766.

Nichols, J.T., Pan, L., Moens, C.B., Kimmel, C.B., 2013. barx1 represses joints and promotes cartilage in the craniofacial skeleton. Development 140, 2765–2775.

Nie, X., Luukko, K., Kettunen, P., 2006. FGF signalling in craniofacial development and developmental disorders. Oral Diseases 12, 102–111.

Nissen, R.M., Yan, J., Amsterdam, A., Hopkins, N., Burgess, S.M., 2003. Zebrafish foxi one modulates cellular responses to Fgf signaling required for the integrity of ear and jaw patterning. Development 130, 2543–2554.

Ornitz, D.M., Itoh, N., 2001. Fibroblast growth factors. Genome Biology 2(Reviews 3001–3005, 3012).

Ornitz, D.M., Xu, J., Colvin, J.S., McEwen, D.G., MacArthur, C.A., Coulier, F., Gao, G., Goldfarb, M., 1996. Receptor specificity of the fibroblast growth factor family. Journal of Biological Chemistry 271, 15292–15297.

Ota, S., Tonou-Fujimori, N., Nakayama, Y., Ito, Y., Kawamura, A., Yamasu, K., 2010. FGF receptor gene expression and its regulation by FGF signaling during early zebrafish development. Genesis 48, 707–716.

Piotrowski, T., Nusslein-Volhard, C., 2000. The endoderm plays an important role in patterning the segmented pharyngeal region in zebrafish (*Danio rerio*). Developmental Biology 225, 339–356.

Robu, M.E., Larson, J.D., Nasevicius, A., Beiraghi, S., Brenner, C., Farber, S.A., Ekker, S.C., 2007. p53 activation by knockdown technologies. PLoS Genetics 3, e78.

Rohner, N., Bercsenyi, M., Orban, L., Kolanczyk, M.E., Linke, D., Brand, M., Nusslein-Volhard, C., Harris, M.P., 2009. Duplication of fgfr1 permits Fgf signaling to serve as a target for selection during domestication. Current Biology 19, 1642–1647.

Sakaguchi, T., Kikuchi, Y., Kuroiwa, A., Takeda, H., Stainier, D.Y., 2006. The yolk syncytial layer regulates myocardial migration by influencing extracellular matrix assembly in zebrafish. Development 133, 4063–4072.

Schilling, T.F., Kimmel, C.B., 1994. Segment and cell type lineage restrictions during pharyngeal arch development in the zebrafish embryo. Development 120, 483–494.

Schilling, T.F., Piotrowski, T., Grandel, H., Brand, M., Heisenberg, C.P., Jiang, Y.J., Beuchle, D., Hammerschmidt, M., Kane, D.A., Mullins, M.C., van Eeden, F.J., Kelsh, R.N., Furutani-Seiki, M., Granato, M., Haffter, P., Odenthal, J., Warga, R.M., Trowe, T., Nusslein-Volhard, C., 1996. Jaw and branchial arch mutants in zebrafish I: branchial arches. Development 123, 329–344.

Scholpp, S., Groth, C., Lohs, C., Lardelli, M., Brand, M., 2004. Zebrafish fgfr1 is a member of the fgf8 synexpression group and is required for fgf8 signalling at the midbrain–hindbrain boundary. Development Genes and Evolution 214, 285–295.

Sperber, S.M., Dawid, I.B., 2008. barx1 is necessary for ectomesenchyme proliferation and osteochondroprogenitor condensation in the zebrafish pharyngeal arches. Developmental Biology 321, 101–110.

Sperber, S.M., Saxena, V., Hatch, G., Ekker, M., 2008. Zebrafish dlx2a contributes to hindbrain neural crest survival, is necessary for differentiation of sensory ganglia and functions with dlx1a in maturation of the arch cartilage elements. Developmental Biology 314, 59–70.

Thisse, B., Thisse, C., 2005. Functions and regulations of fibroblast growth factor signaling during embryonic development. Developmental Biology 287, 390–402.

Thummel, R., Bai, S., Sarras Jr., M.P., Song, P., McDermott, J., Brewer, J., Perry, M., Zhang, X., Hyde, D.R., Godwin, A.R., 2006. Inhibition of zebrafish fin regeneration using *in vivo* electroporation of morpholinos against fgfr1 and msxb. Developmental Dynamics 235, 336–346.

Tissier-Seta, J.P., Mucchielli, M.L., Mark, M., Mattei, M.G., Goridis, C., Brunet, J.F., 1995. Barx1, a new mouse homeodomain transcription factor expressed in cranio-facial ectomesenchyme and the stomach. Mechanisms of Development 51, 3–15.

Tonou-Fujimori, N., Takahashi, M., Onodera, H., Kikuta, H., Koshida, S., Takeda, H., Yamasu, K., 2002. Expression of the FGF receptor 2 gene (fgfr2) during embryogenesis in the zebrafish Danio rerio. Mechanisms of Development 119S, S173–S178.

Trokovic, N., Trokovic, R., Mai, P., Partanen, J., 2003. Fgfr1 regulates patterning of the pharyngeal region. Genes and Development 17, 141–153.

Trueb, B., Taeschler, S., 2006. Expression of FGFRL1, a novel fibroblast growth factor receptor, during embryonic development. International Journal of Molecular Medicine 17, 617–620.

Walshe, J., Mason, I., 2003. Fgf signalling is required for formation of cartilage in the head. Developmental Biology 264, 522–536.

Westerfield, M., 2007. The Zebrafish Book: A Guide for the Laboratory Use of Zebrafish (*Danio rerio*)5th EditionUniversity of Oregon Press, Eugene.

Woo, J., Miletich, I., Kim, B.M., Sharpe, P.T., Shivdasani, R.A., 2011. Barx1-mediated inhibition of Wnt signaling in the mouse thoracic foregut controls tracheo-esophageal septation and epithelial differentiation. PLoS One 6, e22493.

Yan, Y.L., Miller, C.T., Nissen, R.M., Singer, A., Liu, D., Kirn, A., Draper, B., Willoughby, J., Morcos, P.A., Amsterdam, A., Chung, B.C., Westerfield, M., Haffter, P., Hopkins, N., Kimmel, C., Postlethwait, J.H., 2002. A zebrafish sox9 gene required for cartilage morphogenesis. Development 129, 5065–5079.

Yan, Y.L., Willoughby, J., Liu, D., Crump, J.G., Wilson, C., Miller, C.T., Singer, A., Kimmel, C., Westerfield, M., Postlethwait, J.H., 2005. A pair of Sox: distinct and overlapping functions of zebrafish sox9 co-orthologs in craniofacial and pectoral fin development. Development 132, 1069–1083.

Zhang, X., Ibrahimi, O.A., Olsen, S.K., Umemori, H., Mohammadi, M., Ornitz, D.M., 2006. Receptor specificity of the fibroblast growth factor family. The complete mammalian FGF family. Journal of Biological Chemistry 281, 15694–15700.